Signal Processing 176 (2020) 107714

Contents lists available at ScienceDirect

Signal Processing

journal homepage: www.elsevier.com/locate/sigpro

The histogram Poisson, labeled multi-Bernoulli multi-target tracking filter

Leonardo Cament[a,*], Javier Correa[a], Martin Adams[a], Claudio Pérez[a]

Dept. Electrical Engineering & Advanced Mining Technology Center (AMTC), Universidad de Chile, Av. Tupper 2007, 837-0451 Santiago

ARTICLE INFO

Article history:
Received 28 January 2020
Revised 19 May 2020
Accepted 17 June 2020
Available online 7 July 2020

Keywords:
Finite Set Statistics
Target Tracking
Multi-Bernoulli
Poisson birth model

ABSTRACT

A Random Finite Set (RFS) based multi-target filter is proposed, which utilizes a labeled Multi-Bernoulli distribution to model the multi-target state, together with a Poisson RFS distribution to model target birth. Referred to as the Poisson Labeled Multi-Bernoulli (PLMB) filter, results show that, in simulated environments, it outperforms the Labeled Multi-Bernoulli (LMB), δ-Generalized Labeled Multi-Bernoulli (δ-GLMB) and Labeled Multi-Bernoulli Mixtures (LMBM) filters under general target birth scenarios. An algorithm based on a histogram of Gibbs samples is also proposed which efficiently generates a posterior labeled Multi-Bernoulli distribution in a simple manner using a histogram of the state-measurement associations obtained by a Gibbs sampler. The histogram approach is readily applicable to all Multi-Bernoulli based filters and is demonstrated in the form of the Histogram-PLMB (HPLMB) filter.

1. Introduction

Multi-target tracking is a problem of great interest in many engineering applications, ranging from surveillance to safety enforcement and autonomous robotics [1–4]. Different solutions have been proposed, such as the Multiple Hypothesis Tracking (MHT) and Joint Probabilistic Data Association (JPDA) filters [5–7]. To formulate the multi-target tracking problem in a Bayesian manner, in which target cardinality, as well as state, can be jointly estimated, Mahler used Random Finite Set (RFS) and developed the Finite Set Statistical (FISST) framework [8,9]. By using RFS and FISST, the problem of Bayesian multi-object estimation can be expressed in a rigorous manner. As with all multi-target, multi-object tracking formulations, a key issue is the combinatorial nature of the problem, which makes tractable solutions for real-world problems an ongoing research field.

The recently introduced δ-Generalized Labeled Multi-Bernoulli (δ-GLMB) filter proposed by Vo et al. [10,11], which introduces the notion of labeled RFS, is the first true multi-target tracking, closed form solution of the Bayes recursion. It is a true tracking filter in that it uniquely identifies and maintains the track identities of the targets jointly with the estimates of the states within the Bayesian recursion. Although the δ-GLMB filter is analytically exact, it can be intractable due to the combinatorial nature of the posterior solution, and approximations must often be made. It was shown that the truncated distribution is a good approximation of the true posterior distribution using the $\mathcal{L}_1$ norm [11]. The truncation process proposed in [11] relied on extracting the k best assignments between tracks and measurements via the use of Murty's algorithm [12], which still resulted in a high computational complexity. To reduce this complexity, a δ-GLMB filter based on Gibbs-sampling of the posterior RFS distribution was introduced [13]. As a result, the multi-target posterior can be approximated with complexity $\mathcal{O}(MN^2S)$, i.e. linear in the number of measurements M, and quadratic in the number of targets N, for S samples per time step.

A multi-target density, which is related to the δ-GLMB distribution, is the Labeled Multi-Bernoulli (LMB) density [14]. The advantage of the LMB with respect to the δ-GLMB density is that it requires fewer parameters to model the posterior multi-target distribution at the expense of the loss of information related to the correlations between the target association maps. However the gain in computational tractability due to this reduction of the parameters has been shown to outweigh the loss in multi-target state estimation accuracy in many applications. Based on this distribution, Reuter et al. first proposed the LMB filter based on Murty's algorithm [14], and later based on Gibbs-sampling [15]. An implementation of the LMB filter, which utilized Loopy Belief Propagation (LBP) was introduced in [16] with linear computational complexity $\mathcal{O}(MNI)$ with respect to the numbers of measurements M, targets N and LBP iterations I.

* Corresponding author.
E-mail addresses: lcament@ing.uchile.cl (L. Cament), javier.correa@amtc.cl (J. Correa), martin@ing.uchile.cl (M. Adams), clperez@ing.uchile.cl (C. Pérez).

https://doi.org/10.1016/j.sigpro.2020.107714
0165-1684/

Nomenclature

$\mathcal{X}, \mathcal{Y}, \mathcal{B}, \mathcal{Z}, \Phi, \mathcal{L}$	Random Finite Sets (RFSs) modeling the multi-object state, multi-object state of detected targets, appearance of new targets, observations, clutter measurements and target labels (identities), respectively.
X, Y, B, Z, L	Realizations of the RFS representing the multi-object state, multi-object state of detected targets, multi-object state of birth targets, measurement set and target label set, respectively.
$Z_{1:t}$	Collection of set-valued observations up to and including time step t.
$\mathbf{x}$, $\mathbf{z}$	Vector representations of a single-target state and observation.
$\mathbf{F}$, $\mathbf{Q}$, $\mathbf{H}$, $\mathbf{R}$	Matrices representing the linear transition model, transition noise, linear observation model and observation noise.
$G_{\mathcal{X}}[h]$	Probability Generating Functional of the RFS $\mathcal{X}$.
$D_{\mathcal{X}}(\mathbf{x})$	First moment, or intensity function, of the RFS $\mathcal{X}$.
P_S, P_D	Probabilities of target survival and detection.
l_x, l_z	State transition and observation likelihood functions.
ℓ	Target label.
$\mathring{\mathbf{x}}$	Labeled state $\mathring{\mathbf{x}} = (\mathbf{x}, \ell)$.
ω_σ	Weight of a component of a multi-Bernoulli (MB) mixture (MBM) density, representing target set partition σ. ω_N, ω_M, ω_D represent the weights of new, misdetected and detected targets respectively.
r	Probability of existence of an element of a MB based RFS.
f	Probability density function of a target.
$\cdot_{\ell,N}$, $\cdot_{\ell,D}$, $\cdot_{\ell,M}$	Variables $(\cdot)$ corresponding to new, detected and misdetected targets, with label ℓ.
$\cdot_{\sigma,\ell}$	Variable $(\cdot)$ corresponding to target ℓ for partition σ of a MBM density. $(\cdot)$ can be r or f.
$\cdot'$, $\cdot^+$	Predicted and updated variable. Variable $(\cdot)$ can be r, f or G.

Recently in the RFS multi-target tracking literature, multi-Bernoulli filters that utilize a Poisson process birth model have been proposed [17–20]. However, in the article [21], Mahler specified the properties necessary for the distribution of a labeled RFS (LRFS), and stated that a Poisson RFS does not have the necessary properties to be considered to be a true LRFS. In [10, p.4], Vo et al. defined a labeled Poisson RFS and a procedure to generate a finite set of augmented states with distinct labels, but noted that the set of labeled states is not a Poisson RFS. Mahler [21] stated that label-augmented-Poisson Multi-Bernoulli Mixture (PMBM) and hybrid-unlabeled-labeled-PMBM filters are theoretically and physically questionable, because of conflicts between the simultaneous existence of the undetected-density component and the detected-density component. Therefore, this article adopts an unlabeled Poisson RFS distribution which models birth targets (not undetected targets) without identities and a labeled Multi-Bernoulli (MB) distribution which models target tracks - i.e. target identities. It demonstrates that it is possible to design a labeled Bayesian filter based on these concepts, which forbids state-sets with non-distinct labels.

The advantages of using a Poisson process birth model within LMB filters include:

- The ability to model the birth of *any number* of targets at a given time step, whereas an LMB birth density can only model a number, which is limited by the cardinality of the LMB birth density[1].
- The ability to model a birth *rate*, thus allowing filter predictions with varying time steps. This was used in [23] for a multi-sensor scenario where sensor measurements arrived asynchronously.

This article therefore derives a Poisson Labeled Multi-Bernoulli (PLMB) filter based on a Poisson birth model (with unlabeled target state) and an LMB target model (with labeled target state). A motivation for using a Poisson birth distribution is based on [18], where it was shown that a MB distribution naturally results when applying Bayes theorem to a Poisson prior distribution with the standard measurement model defined in [8, p.311]. The PLMB filter assumes a prior LMB density, and after the prediction stage incorporates a Poisson birth model, yielding a PLMB density. Note that in contrast to [18], the Poisson component models birth, but not undetected targets. After update, the filter again yields a posterior which is purely an LMB density. The article offers the following contributions:

1. It is shown that a labeled multi-Bernoulli mixture density can be approximated by an LMB density in a manner similar to which an LMB density has been used to approximate a δ-GLMB density [15]. This maintains the same advantage that the LMB filter has over its δ-GLMB counterpart, in that the number of parameters necessary to model the posterior distribution in the PLMB filter is significantly reduced compared to those necessary in a fully labeled multi-Bernoulli mixture filter. Despite the theoretical loss of correlation information, it is shown that the PLMB filter has multi-target errors similar to the multi-Bernoulli mixture based δ-GLMB and LMB mixture filters, while achieving lower computational times, similar to the LMB filter. An explicit derivation of the MB parameters is given together with two implementation techniques in Sections 4.4 and 4.5.
2. It will be shown that, in the PLMB filter, it is possible to identify each component with a unique track identifier (label) allowing track identities to be initialized and maintained.
3. An efficient PLMB filter, which creates the posterior LMB density based on a histogram of the samples obtained by applying a Gibbs sampler to a cost matrix, as in the sense of [13], is proposed. This is referred to as the Histogram PLMB (HPLMB) filter. In contrast to state of the art LMB filter implementations, the LMB density of the HPLMB filter does not require the approximation of the posterior labeled multi-Bernoulli mixture distribution component. Instead it computes the parameters of the posterior LMB distribution directly from the prior distribution.
4. The proposed histogram based procedure of the PLMB filter uses all the LMB components generated by the Gibbs sampler, circumventing the necessity of identifying and removing repeated components.

Section 2 presents the theoretical background necessary for deriving Bayesian RFS filters. The PLMB filter is derived in Section 3 with two implementation methods being described in Section 4. In Section 5 simulated results are presented giving comparisons with the LMB, δ-GLMB, Labeled Multi-Bernoulli Mixture (LMBM), PMBM and the LBP-PLMB filters. Finally, in Section 6 conclusions are drawn.

[1] Note that versions of the δ-GLMB and LMB filters exist, which create LMB birth densities according to an adaptive birth model based on applying inverse measurement models to the measurements from previous time steps [22].

2. Theoretical background: bayesian recursion with random finite sets

This section reviews the basic RFS concepts and introduces how filter prediction and correction steps are implemented using RFS for multi-target tracking. For a complete description, the reader is referred to [8]. This serves as a prerequisite for the derivation of the PLMB filter given in Section 3.

2.1. Random Finite Sets Overview

An RFS, $\mathcal{X}$, is a random variable, which has instantiations as finite sets $X = \{\mathbf{x}_1, \ldots, \mathbf{x}_n\}$, with $n \geq 0$, $n = 0$ indicating the empty set. Two sources of uncertainty are present in an RFS, namely the unknown number of elements and the uncertainty in the value of each element in the set. An RFS can be described by its probability density function (pdf) $f(X;\ \Theta)$ with Θ being the parameters of the pdf, or alternatively by its Probability Generating Functional (PGFl) $G_{\mathcal{X}}[h]$ defined as:

$$G_{\mathcal{X}}[h] = \int h^X f(X)\delta X. \tag{1}$$

The integration is carried out using the set-integral[2] and h^X is defined as:

$$h^X = \begin{cases} 1 & \text{if } X = \emptyset \\ \prod_{\mathbf{x}\in X} h(\mathbf{x}) & \text{otherwise,} \end{cases} \tag{2}$$

with $0 \leq h(\mathbf{x}) \leq 1$ being a function defined in the space of the individual elements. The PGFl can also be used to calculate the expected value (or first moment) $D_{\mathcal{X}}(\mathbf{x})$ of the multi-target distribution:

$$D_{\mathcal{X}}(\mathbf{x}) = \frac{\delta}{\delta\{\mathbf{x}\}} G_{\mathcal{X}}[h]\bigg|_{h=1}, \tag{3}$$

where $\frac{\delta}{\delta\{\mathbf{x}\}} G_{\mathcal{X}}[h]$ is the functional derivative of $G_{\mathcal{X}}[h]$ [8].

Commonly used distributions in RFS approaches are the Poisson and Bernoulli densities. The Poisson density is given by:

$$f^{\mathrm{p}}(X) = e^{-\langle D_{\mathcal{X}}(\mathbf{x}),1\rangle}[D_{\mathcal{X}}(\mathbf{x})]^X, \tag{4}$$

where its first moment $D_{\mathcal{X}}(\mathbf{x}) = \lambda f(\mathbf{x})$, λ represents the expected number of targets and $f(\mathbf{x})$ represents the spatial density. $\langle f(\mathbf{x}), g(\mathbf{x})\rangle = \int f(\mathbf{x})g(\mathbf{x})d\mathbf{x}$ represents the inner product between functions $f(\mathbf{x})$ and $g(\mathbf{x})$. Its PGFl is given by

$$G^{\mathrm{p}}_{\mathcal{X}}[h] = e^{D_{\mathcal{X}}[h-1]}. \tag{5}$$

A Bernoulli density models random sets in such a way that an element is present with probability r or not present with probability $1 - r$. Its density $f^{\mathrm{b}}(\cdot)$ is given by:

$$f^{\mathrm{b}}(X) = \begin{cases} 1 - r & \text{if } X = \emptyset \\ rf(\mathbf{x}) & \text{if } X = \{\mathbf{x}\} \\ 0 & \text{otherwise.} \end{cases} \tag{6}$$

A multi-Bernoulli density with N_{b} components models random sets such that an element of index i is present with probability r_i or not present with probability $1 - r_i$. When present, each element is distributed according to a probability density function $f_i(\mathbf{x})$. The multi-Bernoulli density $f^{\mathrm{mb}}(X)$ is given by the disjoint union of independent Bernoulli processes $f^b_i(X_i)$:

$$f^{\mathrm{mb}}(X) \propto \sum_{X_1 \uplus \ldots \uplus X_n} \prod_{i=1}^{N_{\mathrm{b}}} f^{\mathrm{b}}_i(X_i), \tag{7}$$

where X_1, ..., X_n are all possible disjoint subsets of X, i.e. $\uplus$ is the disjoint union operator. The PGFl of a multi-Bernoulli density is:

$$G^{\mathrm{mb}}_{\mathcal{X}}[h] = \prod_{i=1}^{N_{\mathrm{b}}} \left(1 - r_i + r_i\langle f^{\mathrm{b}}_i(\mathbf{x}), h(\mathbf{x})\rangle\right). \tag{8}$$

The multi-Bernoulli density is usually parameterized with the set of parameters $\Omega = \{(r_1, f_1), \ldots, (r_{N_{\mathrm{b}}}, f_{N_{\mathrm{b}}})\}$.

2.2. Labeled Random Finite Sets

A Labeled Random Finite Set is composed of labeled states $\mathring{\mathbf{x}} = (\mathbf{x}, \ell) \in \mathring{\mathcal{X}} = \mathcal{X} \times \mathcal{L}$. Therefore, a multi-target state of n elements is given by $\mathring{X} = \{(\mathbf{x}_1, \ell_1), ..., (\mathbf{x}_n, \ell_n)\}$ in which, for the set $\mathring{X}$, with kinematic state X, its corresponding labels are $L = \{\ell_1, ..., \ell_n\}$.

For a function $f(\mathring{\mathbf{x}})$, its integral is defined as:

$$\int f(\mathring{\mathbf{x}})d\mathring{\mathbf{x}} = \sum_{\ell\in\mathcal{L}} \int_{\mathcal{X}} f(\mathbf{x}, \ell)d\mathbf{x}, \tag{9}$$

and its PGFl $G_{\mathring{\mathcal{X}}}[\mathring{h}]$ is defined as:

$$G_{\mathring{\mathcal{X}}}[\mathring{h}] = \int \mathring{h}^{\mathring{X}} f(\mathring{X})\delta\mathring{X}, \tag{10}$$

where the integration is carried out using the labeled set-integral[3], with $0 \leq \mathring{h}(\mathbf{x}, \ell) \leq 1$.

A labeled multi-Bernoulli density is characterized by its PGFl [9, p. 456], [24]:

$$G^{\mathrm{lmb}}_{\mathring{\mathcal{X}}}[h] = \prod_{\ell\in L} \left(1 - r_\ell + r_\ell\langle f_\ell(\mathring{\mathbf{x}}), \mathring{h}(\mathring{\mathbf{x}})\rangle\right), \tag{11}$$

where f_ℓ is the single target density of a target with label ℓ. Note that (11) has the same form as the MB PGFl (8).

2.3. The Standard Bayesian Recursive Filter for RFS

Bayesian filtering is composed of two steps. First, the system's state is predicted one time step ahead using only the state transition model of the system:

$$f'(X|Z_{1:t}) = \int l_x(X|X_t) f(X_t|Z_{1:t})\delta X_t, \tag{12}$$

where X_t and X represent the (multi-target) state at time steps t and the state at $t + 1$, respectively, $Z_{1:\,t}$ represents all the observations received until time step t, $l_x(X|X_t)$ represents the state transition model of the system, $f(\cdot)$ represents the prior density at time step t, and $f'(\cdot)$ represents the predicted density at time step $t + 1$. Second is the correction step, where the most recent observation is used to correct the predicted value of the state. Under Bayes theorem:

$$f^+(X|Z_{1:t+1}) \propto l_z(Z|X) f'(X|Z_{1:t}), \tag{13}$$

where $f^+(\cdot)$ is the updated target state density at time step $t + 1$, Z is the observation set at time step $t + 1$ and $l_z(Z|X)$ is the observation model.

To solve Eqs. (12) and (13), the multi-target transition model and the multi-target observation model have to be defined. In this article, the "standard" multi-target *transition* and *observation* models [8, p.313] are adopted. For simplifying the notation, the inner product between single target hypotheses is defined as $\langle f, g\rangle =$

[2] The set integral is defined as follows:

$$\int f(X)\delta X = f(\emptyset) + \sum_{n=1}^{\infty} \frac{1}{n!} \int f(\{\mathbf{x}_1, \ldots, \mathbf{x}_n\})d\mathbf{x}_1 \cdots d\mathbf{x}_n$$

[3] The labeled set-integral is defined as follows:

$$\int f(\mathring{X})\delta\mathring{X} = f(\emptyset) + \sum_{n=1}^{\infty} \frac{1}{n!} \sum_{\ell\in L} \int f(\{\mathbf{x}_1, \ldots, \mathbf{x}_n\})d\mathbf{x}_1 \cdots d\mathbf{x}_n$$

$\int f(\mathbf{x})g(\mathbf{x})d\mathbf{x}$. Using PGFl, Mahler showed that under this "standard" multi-target *transition* model, the resulting distribution of the prediction step $f(X'|Z_{1:t})$ has a PGFl of the form [8]:

$$G'_{\mathcal{X}|\mathcal{Z}_{1:t}}[h] = G_{\mathcal{B}}[h]G_{\mathcal{X}|\mathcal{Z}_{1:t}}[1 - P_S + P_S\langle l_x(\mathbf{x}|\cdot), h\rangle], \tag{14}$$

where $G_{\mathcal{B}}[h]$ and $G_{\mathcal{X}|\mathcal{Z}_{1:t}}[h]$ are the PGFl of the birth process and the previously estimated state distribution, respectively. It should be noted that in the PGFl and inner product expressions, $\mathbf{x}$ is omitted or replaced by a " $\cdot$ ".

Mahler also showed that using the "standard" multi-target *observation* model (or "standard" multi-target likelihood), the distribution of the corrected state, has the following PGFl [8, p.311]:

$$G^{+}_{\mathcal{X}|\mathcal{Z}_{1:t+1}}[h] = \frac{\frac{\delta}{\delta Z}F[h,g]\big|_{g=0}}{\frac{\delta}{\delta Z}F[h,g]\big|_{h=1,g=0}}, \tag{15}$$

where

$$F[h,g] = G_{\Phi}[g]G'_{\mathcal{X}|\mathcal{Z}_{1:t}}[h(1 - P_D + P_D\langle l_z(\mathbf{z}|\mathbf{x}), g\rangle)], \tag{16}$$

where $G_{\Phi}[g]$ and $G'_{\mathcal{X}|\mathcal{Z}_{1:t}}[h]$ are the PGFl of the clutter process and the predicted state distribution, respectively, and $P_D(\mathbf{x})$ and $l_z(\mathbf{z}|\mathbf{x})$ are the probability of detection and the measurement likelihood function for single targets, respectively. From (14) and (15), a PGFl formulation of a Bayesian filter using the "standard" multi-target transition and observation models can be derived. In the following section, the value of $G_{\mathcal{X}}[h]$ will be determined and substituted into Eqs. (14) and (15) to derive the equations of the PLMB filter.

3. Bayesian Recursion of a Labeled Multi-Bernoulli Density with Poisson Birth Model

This section shows that a Poisson birth process yields an MB distribution after the application of Bayes theorem. It will be further shown that, under Bayes theorem, adding distinct labels to the new targets produced by the Poisson state-measurement associations naturally yields an LMB distribution. Consequently, under Bayes theorem, an LMB density prior yields a PLMB density under prediction when a Poisson birth model is used. Bayesian update then yields a mixture of labeled multi-Bernoulli densities.

3.1. Multi-Bernoulli Density Prediction

For a prior LMB density with parameters (r_ℓ, f_ℓ), where $\ell \in L$, the prediction of the LMB density is $r'_\ell = r_\ell\langle P_S, f_\ell\rangle$ and $f'_\ell(\mathbf{x}) = \frac{\langle P_S l_x(\mathbf{x}|\cdot), f_\ell\rangle}{\langle P_S, f_\ell\rangle}$. This prediction step is efficient and equivalent to the Labeled Probability Hypothesis Density (LPHD) filter prediction step in [24] and [20]. It does not need to convert the LMB density into a δ-GLMB density, and reduce it again to an LMB density as in the LMB filter [14].

3.2. Poisson Birth Process

The Poisson birth intensity is given by $D_{\mathcal{B}}(\mathbf{x}) = \lambda_B f_B(\mathbf{x})$, where λ_B is the expected number of targets to be born with spatial distribution $f_B(\mathbf{x})$. The union of Poisson and LMB densities in PGFl form is:

$$G^{\text{plmb}}_{\mathcal{X}}[h] = G^{\text{p}}_{\mathcal{B}}[h]G^{\text{lmb}}_{\mathcal{Y}}[h], \tag{17}$$

where $G^{\text{p}}_{\mathcal{B}}[h]$ is a Poisson PGFl (Eq. 5) and $G^{\text{lmb}}_{\mathcal{Y}}[h]$ an LMB PGFl (Eq. (11)).

3.3. Posterior Density

The Bayesian update of the Poisson multi-Bernoulli PGFl given in (17) yields the following expression (see the Appendix for the direct derivation of the PLMB posterior PGFl):

$$G^{+}_{\mathcal{X}|\mathcal{Z}}[h] \propto \sum_{\sigma} \omega_\sigma \cdot f^{\text{lmb}}_N[h]f^{\text{lmb}}_M[h]f^{\text{lmb}}_D[h]. \tag{18}$$

The weights of the labeled multi-Bernoulli density are given by $\omega_\sigma = \omega_N \times \omega_M \times \omega_D$, where ω_σ appears to depend on the three weights ω_N, ω_M, and ω_D. Three components are identified, $\omega_N f^{\text{lmb}}_N[h]$ corresponding to the new targets resulting from the update of the Poisson component (to be given in Section 3.4). The other two components arise from the update of the LMB prior component, with $\omega_M f^{\text{lmb}}_M[h]$ corresponding to misdetected targets and $\omega_D f^{\text{lmb}}_D[h]$ corresponding to detected targets (both components will be given in Section 3.5). Note that the PGFl of the posterior is of the form:

$$G^{+}_{\mathcal{X}|\mathcal{Z}}[h] = \sum_{\sigma=1}^{N_{\text{lmb}}} \omega_\sigma \prod_{\ell \in L_\sigma} (1 - r_{\sigma,\ell} + r_{\sigma,\ell}\langle f_{\sigma,\ell}, h\rangle), \tag{19}$$

which corresponds to the PGFl of a LMBM density, where σ represents the σth LMB component. Two approximations for the resulting LMBM posterior parameters, which yield the LMB posterior parameters, are given in Sections 4.4 and 4.5.

3.4. Poisson Intensity Update

Suppose that a set of measurements Z^N is received at time step t. Using the "standard" observation model $l_z(\mathbf{z}|\cdot)$, the PGFl of the posterior of the Poisson birth component is given by the following expression (see the first of the product terms corresponding to the birth targets in (57) in the Appendix):

$$G^{+}_{\mathcal{B}|\mathcal{Z}}[h] \propto \prod_{\mathbf{z}_j \in Z^N} D_{\Theta}(\mathbf{z}_j) + \langle D_{\mathcal{B}} l_z(\mathbf{z}_j|\cdot), h\rangle. \tag{20}$$

Using the normalization given in (58), the posterior Poisson PGFl component can be expressed as:

$$G^{+}_{\mathcal{B}|\mathcal{Z}}[h] \propto \omega_N \prod_{\mathbf{z}_j \in Z^N} \left(1 - r^{+}_{j,N} + r^{+}_{j,N}\left\langle f^{+}_{j,N}, h\right\rangle\right), \tag{21}$$

where

$$\omega_N = \prod_{\mathbf{z}_j \in Z^N} D_{\Theta}(\mathbf{z}_j) + \langle D_{\mathcal{B}} l_z(\mathbf{z}_j|\cdot), 1\rangle, \tag{22}$$

$$r^{+}_{j,N} = \frac{\langle D_{\mathcal{B}} l_z(\mathbf{z}_j|\cdot), 1\rangle}{D_{\Theta}(\mathbf{z}_j) + \langle D_{\mathcal{B}} l_z(\mathbf{z}_j|\cdot), 1\rangle}, \quad f^{+}_{j,N}(\mathbf{x}) = \frac{D_{\mathcal{B}}(\mathbf{x}) l_z(\mathbf{z}_j|\mathbf{x})}{\langle D_{\mathcal{B}} l_z(\mathbf{z}_j|\cdot), 1\rangle}. \tag{23}$$

Eq. (21) can be interpreted as a multi-Bernoulli density composed of target hypotheses born from each measurement $z_j \in Z^N$. Labels are defined as $\ell_j = (t, j)$ based on the time t at which they are assigned and the jth measurement used to assign the label. If we assume that measurements are distinct and produced by unique targets, it is possible to establish a mapping between new targets identified by label $\ell \in L = \{(t,1), ..., (t, m = |Z^N|)\}$ and measurements - i.e. $\ell_1 = (t,1) \rightarrowtail z_1$,..., $\ell_m = (t,m) \rightarrowtail z_m$. In implementation, the LMB density can be constructed by including the Kronecker delta function $\delta_{\ell_j}(\ell)$ into the measurement likelihood:

$$l_z(\mathbf{z}_j|\mathbf{x}, \ell) = l_z(\mathbf{z}_j|\mathbf{x})\delta_{\ell_j}(\ell), \quad \text{where} \quad \delta_{\ell_j}(\ell) = \begin{cases} 1 & \ell = \ell_j, \\ 0 & \text{otherwise.} \end{cases} \tag{24}$$

Let $\mathring{B}$ be the labeled target set resulting directly from the Poisson birth set B after update, with $L^N = \mathcal{L}(\mathring{B})$ being subsets of the labels L corresponding to new targets. Then, the posterior MB PGFl can be expressed as:

$$G^{+}_{\mathcal{B}|\mathcal{Z}}[h] \propto \omega_N \underbrace{\prod_{\ell \in L^N} \left(1 - r^{+}_{\ell,N} + r^{+}_{\ell,N}\left\langle f^{+}_{\ell,N}, h\right\rangle\right)}_{f^{\text{lmb}}_N[h]}, \tag{25}$$

where

$$\omega_N = \prod_{\ell \in L^N} D_\Theta(\mathbf{z}_{j_\ell}) + \langle D_\mathcal{B} l_z(\mathbf{z}_{j_\ell}|\cdot), 1\rangle, \tag{26}$$

$$r^+_{\ell,N} = \frac{\langle D_\mathcal{B} l_z(\mathbf{z}_{j_\ell}|\cdot), 1\rangle}{D_\Theta(\mathbf{z}_{j_\ell}) + \langle D_\mathcal{B} l_z(\mathbf{z}_{j_\ell}|\cdot), 1\rangle}, \quad f^+_{\ell,N}(\mathbf{x}) = \frac{D_\mathcal{B}(\mathbf{x}) l_z(\mathbf{z}_{j_\ell}|\mathbf{x}, \ell)}{\langle D_\mathcal{B} l_z(\mathbf{z}_{j_\ell}|\cdot), 1\rangle}. \tag{27}$$

By construction, the labels are distinct. Mathematically, when $f^{\text{mb}}(\mathring{X})$ is evaluated with a label $\ell \notin L$, $\delta_{\ell_j}(\ell) = 0$, thus $f^{\text{mb}}(\mathring{X}) = 0$. Therefore the resulting MB density is a true LMB density.

3.5. Labeled Multi-Bernoulli Density Update

The update of the prior LMB component in (17) corresponds to a sum of LMB terms composed of $\omega_M f^{\text{lmb}}_M[h]$ and $\omega_D f^{\text{lmb}}_D[h]$, as was shown in Eq. (18). The parameters of the LMB component representing misdetected targets are given by:

$$\omega_M = \prod_{\ell^M \in L^M} \left(1 - r'_{\ell^M} + r'_{\ell^M} \left\langle (1 - P_D) f'_{\ell^M}, 1 \right\rangle\right), \tag{28}$$

$$f^{\text{lmb}}_M[h] = \prod_{\ell^M \in L^M} \left(1 - r^+_{\ell^M,0} + r^+_{\ell^M,0} \left\langle f^+_{\ell^M,0}, h \right\rangle\right), \tag{29}$$

$$f^+_{\ell^M,0}(\mathbf{x}) = \frac{(1 - P_D(\mathbf{x})) f'_{\ell^M}(\mathbf{x})}{\left\langle (1 - P_D) f'_{\ell^M}, 1 \right\rangle}, \quad r^+_{\ell^M,0} = \frac{r'_{\ell^M} \left\langle (1 - P_D) f'_{\ell^M}, 1 \right\rangle}{1 - r'_{\ell^M} + r'_{\ell^M} \left\langle (1 - P_D) f'_{\ell^M}, 1 \right\rangle}, \tag{30}$$

and the parameters of the LMB component representing detected targets are given by:

$$\omega_D = \prod_{\ell^D \in L^D} r'_{\ell^D} \langle P_D l_z(\mathbf{z}_j|\cdot) f'_{\ell^D}, 1\rangle, \tag{31}$$

$$f^{\text{lmb}}_D[h] = \prod_{\ell^D \in L^D} \left(1 - r^+_{\ell^D,j} + r^+_{\ell^D,j} \left\langle f^+_{\ell^D,j}, h \right\rangle\right), \tag{32}$$

$$f^+_{\ell^D,j}(\mathbf{x}) = \frac{P_D(\mathbf{x}) l_z(\mathbf{z}_j|\mathbf{x}) f'_{\ell^D}(\mathbf{x})}{\langle P_D l_z(\mathbf{z}_j|\cdot) f'_{\ell^D}, 1\rangle}, \quad r^+_{\ell^D,j} = 1, \tag{33}$$

where $L^M = \mathcal{L}(\mathring{Y}^M)$ represents the labels of the target hypotheses that were misdetected, and $L^D = \mathcal{L}(\mathring{Y}^D)$ represents the labels of the detected target hypotheses, corresponding to measurements Z^D.

3.6. Target Track Propagation

Each multi-Bernoulli component in the mixture of (19) can be interpreted as a possible configuration of the multi-target state. Each target hypothesis is identified with a unique label which has the following properties **P1** and **P2**:

- **P1**: Within a multi-Bernoulli component, all labels are unique.
- **P2**: A track identity is maintained between different multi-Bernoulli components and different time-steps.

Given the observation model described in Section 2.3, since each target can generate at most one observation at a time, if $|Z|$ observations correspond to targets (they do not correspond to clutter), then $|Z|$ different targets are assumed to have generated those observations. The proposed algorithm identifies an observation as (potentially) coming from a target on two occasions: 1) When a new MB component is created from the birth model or; 2) When the state of an existing LMB component is corrected.

Proposition 1. *A target identified by the pair (t, j), where j is the index of the j-th measurement used to initialize the component at time-step t (using Eq. (24)), has properties **P1** and **P2**.*

Proof of Proposition 1. Property **P2** can be guaranteed since the proposed definition of the identity of tracks makes reference to the time and measurement index in which the track was created. Therefore the identity of a track is always maintained.

By induction, at time-step 1, when no prior target existed, the PGFl after the filter is executed is of the form of Eq. (21), identifying every created target with the pair $(t = 1, j)$, which has property **P1**. Assuming that properties **P1** and **P2** are maintained after T iterations of the filter, when a single iteration of the filter is then applied, multiple Bernoulli components are created. Note that, from Eq. (18), the different components of the mixture are created using disjoint subsets of prior components and disjoint subsets of the newly received measurements to either update prior components or create new components. Since these partitions are disjoint, a prior component cannot be repeated within a mixture component. Taking into consideration the newly created targets, which differ in the time t component, property **P1** is maintained.

Since the track identification makes reference to the time the track was initialized, they maintain track identity between time-steps and in different components of the mixture, thus having property **P2**. □

4. Histogram Poisson Labeled Multi-Bernoulli (HPLMB) Filter Implementation

In this work, in order to achieve faster computing times, a single LMB density is used as an approximation of the posterior LMBM density.

4.1. Weight Simplification

In order to reduce the number of weight components, $\omega_{\tilde{N}}$ is defined as

$$\omega_{\tilde{N}} = \prod_{\mathbf{z} \in Z^D} D_\Theta(\mathbf{z}_j) + \langle D_\mathcal{B} P_D l_z(\mathbf{z}|\cdot), 1\rangle. \tag{34}$$

The simplification of weight ω_σ is then obtained by multiplying and dividing it by $\omega_{\tilde{N}}$:

$$\begin{aligned}\omega_\sigma &= \underbrace{\left(\omega_N \times \omega_{\tilde{N}}\right)}_{\text{constant } \forall \sigma} \times \omega_M \times \underbrace{\left(\frac{\omega_D}{\omega_{\tilde{N}}}\right)}_{\omega'_D}, \quad \propto \omega_M \times \omega'_D, \\ &= \prod_{\ell^M \in Y^M} \left(1 - r_{\ell^M} + r_{\ell^M} \langle (1 - P_D) f_{\ell^M}, 1\rangle\right) \\ &\quad \times \prod_{\ell^D \in Y^D} \frac{r_{\ell^D} \left\langle P_D l_z(\mathbf{z}_{j_{\ell^D}}|\cdot) f_{\ell^D}, 1 \right\rangle}{D_\Theta(\mathbf{z}_{j_{\ell^D}}) + \langle D_\mathcal{B} l_z(\mathbf{z}_{j_{\ell^D}}|\cdot), 1\rangle},\end{aligned} \tag{35}$$

where the term $\omega_N \times \omega_{\tilde{N}} = [D_\Theta(\mathbf{z}) + \langle D_\mathcal{B} P_D l_z(\mathbf{z}|\cdot), 1\rangle]^Z$ is constant for any partition set. Therefore it can be omitted in the weight calculation. The term ω'_D can be considered to represent the detected target likelihood.

4.2. Ranked Assignment

The posterior density given by its PGFl in Eq. (19), with weight ω_σ given by Eq. (35), is composed of all possible partitions σ. The partition σ is equivalent to an assignment of the matrix $\mathbf{C}$, where the assignment is defined as the set of pairs (i, j) for all rows i, such that there is a bijective function $\mathcal{L}(\cdot)$, in which $\ell = \mathcal{L}(i)$ and columns j, which represent the target-measurement assignment or misdetections. $\mathbf{C}$ is given by

$$\mathbf{C} = \begin{pmatrix} \mathbf{C_D} & \mathbf{C_M} \end{pmatrix}, \tag{36}$$

where, $\mathbf{C_D}$ is an $n \times m$ matrix representing the cost of associating $m = |Z|$ measurements to $n = |Y|$ existing targets (the second

product term in Eq. (35)). $\mathbf{C_M}$ is an $n \times n$ diagonal matrix representing the cost of misdetecting a known target (the first product term in Eq. (35)). Thus, the specific elements (i, j) in each of these matrices are:

$$\mathbf{C_D}[i,j] = \frac{r_i \langle P_D l_z(\mathbf{z}_j|\cdot) f_i, 1 \rangle}{D_\Theta(\mathbf{z}_j) + \langle D_B l_z(\mathbf{z}_j|\cdot), 1 \rangle}, \tag{37}$$

$$\mathbf{C_M}[i,j] = \begin{cases} 1 - r_i + r_i \langle (1 - P_D) f_i, 1 \rangle & i = j \\ 0 & \text{otherwise} \end{cases}. \tag{38}$$

Given an assignment σ of the $\mathbf{C}$ matrix at the current time step, the weight can be obtained as:

$$\omega_\sigma = \prod_{(i,j)\in\sigma} \mathbf{C}[i,j]. \tag{39}$$

It should be noted that, since $\mathbf{C_M}$ is a diagonal matrix, the only possible valid associations of a row i within $\mathbf{C_M}$ is a single value located on its diagonal, which corresponds to the target being misdetected. Note also that all measurements j with no assignment in σ produce a new target with parameters (r, f) given by Eq. (27). Thus, the resulting LMB component will model $n + m$ possible targets (all existing targets plus all possible new targets).

Due to the intractability of maintaining the huge number of posterior components, only a limited number of assignments with the highest weights ω_σ from $\mathbf{C}$ are obtained. State of the art methods to find the highest weights ω_σ, and therefore the associated assignment σ, are Murty's algorithm [12], which solves the k-best assignment problem for the cost matrix $-\log(\mathbf{C})$, and Gibbs sampling used in [13] that samples the assignments σ from the posterior distribution. In this article, the Gibbs sampling method is used because of its linear complexity compared to the cubic complexity of Murty's algorithm with respect to the number of measurements. To further improve the computational efficiency however, a histogram posterior approximation is also introduced. First, the Gibbs sampling process is explained in Section 4.3 followed by the classical posterior approximation in Section 4.4, which yields the PLMB filter, and finally the proposed histogram posterior approximation is given in Section 4.5, yielding the HPLMB filter.

4.3. Gibbs Sampling Procedure for the Update Process

Following [13], it is possible to define a Markov Chain to sample associations from the $\mathbf{C}$ matrix as follows:

$$\omega_\sigma \propto \mathbf{1}_\Gamma(\sigma) \prod_{i=1}^{n} \eta_i(\sigma_i), \tag{40}$$

where, in general, an indicator function $\mathbf{1}_Y(X)$ is defined by:

$$\mathbf{1}_Y(X) = \begin{cases} 1 & X \subseteq Y, \\ 0 & \text{otherwise}, \end{cases} \quad \text{and} \quad \eta_i(\sigma_i) = \begin{cases} \mathbf{C_M}[i,i] & \sigma_i = 0 \\ \mathbf{C_D}[i,\sigma_i] & \text{otherwise}, \end{cases} \tag{41}$$

where σ is a realization of $\mathcal{I}^{\text{lmb}}$ and Γ is the set of positive 1-1 vectors in $\{0{:}\ m\}^n$.

The number of repeated samples produced by the Gibbs sampler is proportional to the weight ω_σ and Vo et al. proved that it converges exponentially, guaranteeing that after only a few iterations, the sampled MB components will be those with the highest weights [13]. The Gibbs sampler must be initialized with a valid realization $\sigma^{(0)}$. Two simple valid realizations for the initialization $\sigma^{(0)}$ could be:

1. All targets correspond to misdetections and all measurements to new targets, or
2. A one-time solution to the optimal ranked assignment explained in Section 4.2, which could be obtained with the Hungarian algorithm [25].

The Gibbs sampling procedure for the PLMB filter is similar to that used in the LMB and δ-GLMB filters. The difference is that Γ, for the LMB and δ-GLMB filters, is a set of 1-1 vectors in $\{-1{:}\ m\}^n$ and represented by separate weights $1 - r$ and $r\langle(1 - P_D)f, 1\rangle$. However in the PLMB filter, Γ is a set of 1-1 vectors in $\{0{:}\ m\}^n$, because the non-surviving and misdetected target likelihoods are combined and represented by a single weight (Eq. (38)). Gibbs sampling is explained in detail in [13].

4.4. Classical Posterior Approximation

Iterating the Gibbs sampler S times yields S possible assignments $\sigma^{(s)}$, $1 \leq s \leq S$. Many of these assignments will be repeated. After the removal of the repeated assignments, N_{lmb} unique assignments remain. The posterior labeled Multi-Bernoulli Mixture (MBM) is then represented by the mixture weights in Eq. (39) and the set $\{(r_{\sigma,\ell}, f_{\sigma,\ell})\}$ corresponding to each assignment σ. Finally the approximated LMB density is represented by:

$$r_\ell = \sum_{\sigma=1}^{N_{\text{lmb}}} \omega_\sigma \mathbf{1}_{L_\sigma}(\ell) r_{\sigma,\ell} \quad \text{and} \quad f_\ell = \sum_{\sigma=1}^{N_{\text{lmb}}} \omega_\sigma \mathbf{1}_{L_\sigma}(\ell) f_{\sigma,\ell}. \tag{42}$$

Note that $\omega_\sigma \mathbf{1}_{L_\sigma}(\ell) = 0$ if $\ell \notin L_\sigma$, where L_σ are the target labels of partition σ.

4.5. Histogram Posterior Approximation

The proposed histogram based procedure uses all the sampled MB components, while avoiding the removal of components, which is necessary in the traditional procedure given in Section 4.4. It proceeds by sampling possible assignments from Eq. (40) and then using these assignments, it calculates the expected value of each hypothesized target's probability of existence and spatial distribution parameters.

To achieve this, the creation of a histogram of the Gibbs samples $\sigma^{(s)}$ is useful, since the number of times an assignment σ is sampled is proportional to the weight of its posterior MB component. The 2D histogram's elements (i, j), where i represents the ith prior target hypothesis and j represents the jth measurement, are given by $H_{i,j}$, which are defined as the number of times that element (i, j) was sampled. Note that $j = 0$ corresponds to a misdetected target hypothesis.

Table 1 shows an example of three target hypotheses and four measurements and how each iteration of the Gibbs sampler (left tables) increases the histogram values $H(i, j)$ (center tables). When an element $(i, j) \in \sigma$ is sampled, a cross $(\times)$ is shown. The left tables show sampled assignments and the center tables show the corresponding histograms at that iteration of the Gibbs sampler. The rows beginning with β represent measurements assigned to new targets. Note that when a sample contains an element $(i, j) \in \sigma$ ($\times$ in the left tables), the corresponding element (i, j) in H (center tables) is incremented by one - i.e. $H(i, j) += 1$, $\forall (i, j) \in \sigma^{(s)}$. The first row shows iteration $s = 0$, where no samples (assignments) yet exist, thus the histogram values are all 0. The second row shows iteration $s = 1$, where the sample (assignment) $\sigma^{(1)}$ is initialized with all target hypotheses as misdetections and all measurements as birth target hypotheses (row β), which corresponds to a unit increment in each corresponding cell in the histogram table H. Finally, after $s = S$ iterations (Gibbs samples), the normalized histogram (or weight) $h_{i,j} = \frac{H(i,j)}{S}$ can be calculated (lower right table). In the example of Table 1, $S = 5$.

Hence, the value of each element (i, j) of $h_{i,j}$, is proportional to the importance of the corresponding single target hypothesis. Then the posterior LMB density component for target $\ell = \mathcal{L}(i)$ is a weighted sum of all single-target densities over the i-th row of $h_{i,j}$. It can be seen that all columns and all rows sum to unity, except column $\emptyset$, because there is no restriction on the number of

Table 1
Example procedure for calculating the histogram for the HPLMB Filter.

$\sigma^{(0)}$	$\emptyset$	$\mathbf{z}_1$	$\mathbf{z}_2$	$\mathbf{z}_3$	$\mathbf{z}_4$
β					
$\mathbf{x}_1$					
$\mathbf{x}_2$					
$\mathbf{x}_3$					

→

H	$\emptyset$	$\mathbf{z}_1$	$\mathbf{z}_2$	$\mathbf{z}_3$	$\mathbf{z}_4$
β		0	0	0	0
$\mathbf{x}_1$	0	0	0	0	0
$\mathbf{x}_2$	0	0	0	0	0
$\mathbf{x}_3$	0	0	0	0	0

$\sigma^{(1)}$	$\emptyset$	$\mathbf{z}_1$	$\mathbf{z}_2$	$\mathbf{z}_3$	$\mathbf{z}_4$
β		×	×	×	×
$\mathbf{x}_1$	×				
$\mathbf{x}_2$	×				
$\mathbf{x}_3$	×				

→

H	$\emptyset$	$\mathbf{z}_1$	$\mathbf{z}_2$	$\mathbf{z}_3$	$\mathbf{z}_4$
β		1	1	1	1
$\mathbf{x}_1$	1	0	0	0	0
$\mathbf{x}_2$	1	0	0	0	0
$\mathbf{x}_3$	1	0	0	0	0

$\sigma^{(2)}$	$\emptyset$	$\mathbf{z}_1$	$\mathbf{z}_2$	$\mathbf{z}_3$	$\mathbf{z}_4$
β			×		×
$\mathbf{x}_1$		×			
$\mathbf{x}_2$	×				
$\mathbf{x}_3$				×	

→

H	$\emptyset$	$\mathbf{z}_1$	$\mathbf{z}_2$	$\mathbf{z}_3$	$\mathbf{z}_4$
β		1	2	1	2
$\mathbf{x}_1$	1	1	0	0	0
$\mathbf{x}_2$	2	0	0	0	0
$\mathbf{x}_3$	1	0	0	1	0

$\sigma^{(3)}$	$\emptyset$	$\mathbf{z}_1$	$\mathbf{z}_2$	$\mathbf{z}_3$	$\mathbf{z}_4$
β					×
$\mathbf{x}_1$		×			
$\mathbf{x}_2$			×		
$\mathbf{x}_3$				×	

→

H	$\emptyset$	$\mathbf{z}_1$	$\mathbf{z}_2$	$\mathbf{z}_3$	$\mathbf{z}_4$
β		1	2	1	3
$\mathbf{x}_1$	1	2	0	0	0
$\mathbf{x}_2$	2	0	1	0	0
$\mathbf{x}_3$	1	0	0	2	0

$\sigma^{(4)}$	$\emptyset$	$\mathbf{z}_1$	$\mathbf{z}_2$	$\mathbf{z}_3$	$\mathbf{z}_4$
β			×		
$\mathbf{x}_1$					×
$\mathbf{x}_2$		×			
$\mathbf{x}_3$				×	

→

H	$\emptyset$	$\mathbf{z}_1$	$\mathbf{z}_2$	$\mathbf{z}_3$	$\mathbf{z}_4$
β		1	3	1	3
$\mathbf{x}_1$	1	2	0	0	1
$\mathbf{x}_2$	2	1	1	0	0
$\mathbf{x}_3$	1	0	0	3	0

$\sigma^{(5)}$	$\emptyset$	$\mathbf{z}_1$	$\mathbf{z}_2$	$\mathbf{z}_3$	$\mathbf{z}_4$
β		×	×		×
$\mathbf{x}_1$	×				
$\mathbf{x}_2$	×				
$\mathbf{x}_3$				×	

→

H	$\emptyset$	$\mathbf{z}_1$	$\mathbf{z}_2$	$\mathbf{z}_3$	$\mathbf{z}_4$
β		2	4	1	4
$\mathbf{x}_1$	2	2	0	0	1
$\mathbf{x}_2$	3	1	1	0	0
$\mathbf{x}_3$	1	0	0	4	0

→

h	$\emptyset$	$\mathbf{z}_1$	$\mathbf{z}_2$	$\mathbf{z}_3$	$\mathbf{z}_4$
β		2/5	4/5	1/5	4/5
$\mathbf{x}_1$	2/5	2/5	0	0	1/5
$\mathbf{x}_2$	3/5	1/5	1/5	0	0
$\mathbf{x}_3$	1/5	0	0	4/5	0

targets which can be misdetected, and row β, because there is no restriction on the number of measurements that can be assigned to birth targets or clutter. However a target must be assigned to either a measurement or a misdetection and a measurement must be assigned to either a target, birth target, or clutter.

Note that by definition $h_{i,0} = 1 - \sum_{j=1}^{m} h_{i,j}$, which represents the proportion of samples for which target ℓ was misdetected, or equivalently, the proportion of assignments using entry $i, n+i$ of the cost matrix $\mathbf{C}$. Similarly, $h_{0,j} = 1 - \sum_{i=1}^{n} h_{i,j}$, which represents the proportion of samples in which measurement j was not associated with any target.

In the posterior MBM distribution, when a target is assigned to a measurement, the probability of existence is $r = 1$, and when the target is misdetected its probability of existence is given by Eq. (30). Therefore, for the PLMB filter, the expected probability of existence for target $\ell = \mathcal{L}(i)$ is calculated as the weighted average using the weights $h_{i,j}$ as:

$$r_\ell^+ = \sum_{j=0}^{m} h_{i,j} r_{\ell,j}^+ = h_{i,0} \frac{r'_\ell \langle (1-P_D) f'_\ell, 1 \rangle}{1 - r'_\ell + r'_\ell \langle (1-P_D) f'_\ell, 1 \rangle} + \left(\sum_{j=1}^{m} h_{i,j} \right),$$
$$= h_{i,0} \frac{r'_\ell \langle (1-P_D) f'_\ell, 1 \rangle}{1 - r'_\ell + r'_\ell \langle (1-P_D) f'_\ell, 1 \rangle} + (1 - h_{i,0}),$$
$$= 1 - \frac{h_{i,0}\left(1 - r'_\ell\right)}{1 - r'_\ell + r'_\ell \langle (1-P_D) f'_\ell, 1 \rangle}. \tag{43}$$

Similarly, when target i is assigned to measurement j, its updated spatial distribution is given by Eq. (33), while when the target is misdetected its updated spatial distribution is given by Eq. (30). Again, the expected spatial distribution is calculated as the weighted average of these expressions:

$$f_\ell^+(\mathbf{x}) = h_{i,0} \frac{(1-P_D(\mathbf{x})) f'_\ell(\mathbf{x})}{\langle (1-P_D) f'_\ell, 1 \rangle} + \sum_{j=1}^{m} h_{i,j} \frac{P_D(\mathbf{x}) l_z(\mathbf{z}_j|\mathbf{x}) f'_\ell(\mathbf{x})}{\left\langle P_D l_z(\mathbf{z}_j|\cdot) f'_\ell, 1 \right\rangle}. \tag{44}$$

Finally, new targets arise from measurements that were not associated with any targets, captured by $h_{0,j}$. From Eq. (23), for each measurement, a new Bernoulli component with label $\ell = (t, j)$, is created with probability of existence and spatial distribution equal

to:

$$r_\ell^+ = h_{0,j}\frac{\langle D_{\mathcal{B}} l_z(\mathbf{z}_j|\cdot),1\rangle}{D_\Theta(\mathbf{z}) + \langle D_{\mathcal{B}} l_z(\mathbf{z}_j|\cdot),1\rangle},\quad f_\ell^+(\mathbf{x}) = \frac{D_{\mathcal{B}}(\mathbf{x}) l_z(\mathbf{z}_j|\mathbf{x})}{\langle D_{\mathcal{B}} l_z(\mathbf{z}_j|\cdot),1\rangle}, \tag{45}$$

respectively. This posterior approximation results in the HPLMB filter to be demonstrated in the results.

4.6. Discussion

It was shown that each component of the mixture is a PGFl of a LMB distribution, thus the full mixture and its truncated versions are both mixtures of labeled multi-Bernoulli PGFl.

The methodology used in the LMB filter [15] needs to use the Gibbs sampler S times, and the resulting posterior labeled MBM is composed of repeated LMB components that must be identified and removed, obtaining a total of $N^{\text{lmb}} \leq S$ LMB components. The proposed histogram based procedure uses all the sampled LMB components, circumventing the necessity of identifying and removing components, thus providing an efficient implementation method.

It can be seen that the probability of existence $r_{\ell,j}^+$ in the first row of (43) is equivalent to the LMB updated probability of existence in [15, Eq. 19], except for the term $r_{\ell,0}^+$.

5. Experimental Results

In this section simulated results using the proposed Gibbs sampled PLMB (Section 4.4) and HPLMB (Section 4.5) filters are shown and comparisons are made with the Gibbs sampled versions of the LMB [15], δ-GLMB [13,26], LMBM [24], PMBM [20] filters, as well as an LBP implementation of the PLMB filter. This is carried out in a manner similar to [27], except that in [27], several Murty's algorithm based MB filters were compared. The results here are compared using the Optimal Sub-Pattern Assignment (OSPA) [28] and OSPA$^{(2)}$ [29] metrics and the Multi Object Tracking Precision (MOTP) and Multi Object Tracking Accuracy (MOTA) CLEAR MOT metrics [30]. Both the OSPA and OSPA$^{(2)}$ metrics measure the precision and cardinality of two sets of targets (ground truth and estimates in this case). The MOTP metric gives the estimated target location errors, when correctly detected, and the MOTA metric gives the accuracy in tracking targets, taking into account misdetections, false alarms and label switching.

5.1. Multi-Target State Extraction

5.1.1. State Extraction for the LMB, PLMB, LBP-PLMB & HPLMB Filters

The final position estimates of the LMB, PLMB, LBP-PLMB and HPLMB filters are obtained via Maximum A Posteriori (MAP) estimation using the following procedure: 1) The cardinality distribution $\rho(n)$ of the LMB component of the filters is calculated; 2) The most probable cardinality is chosen as the number of targets N_ρ; 3) The target hypotheses f_ℓ with the highest N_ρ probabilities of existence are selected as targets; 4) Individual target hypotheses are modeled as a Gaussian mixture $f_\ell(\mathbf{x}) = \sum_{\iota=1}^{N_\ell^g} \omega_{\ell,\iota}\mathcal{N}(\mathbf{x}; m_{\ell,\iota}, \Sigma_{\ell,\iota})$. For each target f_ℓ, $\ell \in L$, the final target estimate is selected as the mean value of the Gaussian distribution with the highest weight, i.e., $\hat{x}_\ell = m_{\ell,\text{argmax}(\omega_{\ell,\iota})}$.

5.1.2. State Extraction for the LMBM and PMBM Filters

For final state extraction, the MBM component of the PMBM density is converted to a MB density as shown in Eqs. (42). In the same manner, the LMBM density is reduced to an LMB density, and the same multi-target state extraction method used for the LMB filter is adopted.

5.1.3. State Extraction for the δ-GLMB Filter

The final target estimates in the δ-GLMB filter are extracted as follows: 1) The cardinality distribution $\rho(n)$ of the MB component of the filters is calculated; 2) The most probable cardinality is chosen as the number of targets N_ρ; 3) All the MB components with cardinality N_ρ are selected; 4) The MB component with the highest weight is selected; 5) For each target $f_\ell, \ell \in L$, its final estimate is given by $\hat{x}_\ell = m_{\ell,\text{argmax}(\omega_{\ell,\iota})}$.

5.2. Simulated Results

As a proof of concept, Fig. 1 shows a simulated scenario composed of 20 independent tracks, which initiated and terminated at different times. The time steps for the appearance of new targets are $t = 1$ (5 targets), $t = 20$ (9 targets), $t = 40, 60, 80$ (2 targets each).

The states of the moving targets are composed of their positions and velocities in 2-dimensional space, $\mathbf{x}_t = [x_t, y_t, \dot{x}_t, \dot{y}_t]$. A single-target state for target ℓ is modeled by a Gaussian mixture with N_ℓ^g components, $f_\ell(\mathbf{x}) = \sum_{\iota=1}^{N_\ell^g} \omega_{\ell,\iota}\mathcal{N}(\mathbf{x}; m_{\ell,\iota}, \Sigma_{\ell,\iota})$. A constant velocity model is assumed as the motion model and the observation model measures the Cartesian position of targets in the environment. Both models can be written in linear form using the following motion ($\mathbf{F}$) and observation ($\mathbf{H}$) matrices:

$$\mathbf{F} = \begin{bmatrix} 1 & 0 & \Delta t & 0 \\ 0 & 1 & 0 & \Delta t \\ 0 & 0 & 1 & 0 \\ 0 & 0 & 0 & 1 \end{bmatrix}, \quad \mathbf{H} = \begin{bmatrix} 1 & 0 & 0 & 0 \\ 0 & 1 & 0 & 0 \end{bmatrix}, \tag{46}$$

where $\Delta t = 1$ [s] is the sampling time, and the covariance matrices of the motion noise $\mathbf{Q}$ and the measurement noise $\mathbf{R}$ are as follows:

$$\mathbf{Q} = 5.0^2\,\mathbf{q}\,\mathbf{q}^T,\ \mathbf{R} = 10.0^2\,\mathbf{I}_{2\times 2},\ \mathbf{q}^T = \begin{bmatrix} 0.5\Delta t^2 & 0 & \Delta t & 0 \\ 0 & 0.5\Delta t^2 & 0 & \Delta t \end{bmatrix}, \tag{47}$$

with $\mathbf{I}$ being the identity matrix.

All filters have the following parameters: Probability of survival: $P_S = 0.99$; Probability of detection: $P_D = 0.98$; Uniformly distributed clutter with average rate $\lambda_c = 30$ per scan; The region of

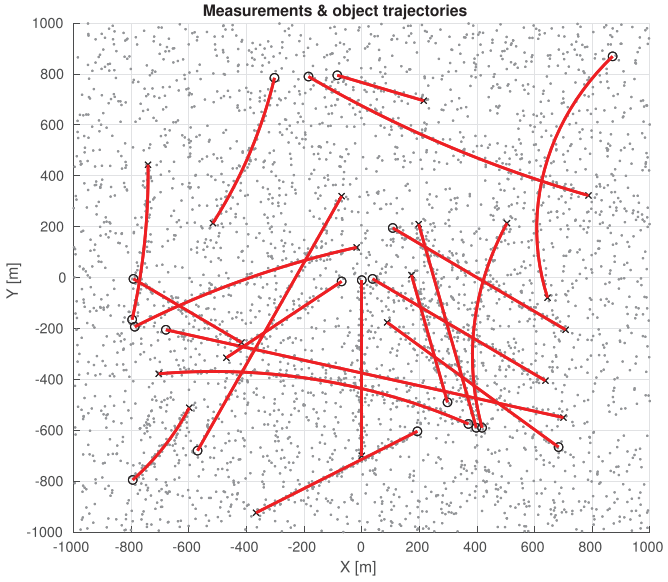

Fig. 1. Ground truth trajectories, starting at positions marked with the symbol "$\circ$", and ending at positions marked with symbol " $\times$ ". The gray dots show the superimposed measurements (including clutter) acquired during the 100 time steps.

Table 2
Filter parameters used in the experiments.

Parameter		Applicable to filters:
Number of iterations of Gibbs sampler	$S = 1,000$	All, except LBP-PLMB
Limit on number of posterior components	$N^{\text{mb}} \leq 1,000$	δ-GLMB, LMBM & PMBM
Pruning threshold for components	$\omega_k \geq 10^{-15}$	δ-GLMB, LMBM & PMBM
Maximum number of tracks	$N^{\text{b}} \leq 100$	LMB, PLMB, LBP-PLMB & HPLMB
Threshold to prune tracks	$r_\ell \geq 10^{-3}$	All, except δ-GLMB
Max. no. Gaussian components in each track	$N_\ell^g \leq 10$	All
Pruning threshold for Gaussian comps. per track	$\omega_{\ell,\iota} \geq 10^{-5}$	All
Merging threshold for Gaussian comps. per track	4	All

interest is between the bounds $[-1000, 1000]$[m] for the x and y axes.

To demonstrate the possible advantages and disadvantages of the Poisson and MB birth models, the simulations are executed with three different birth configurations:

1. A single Gaussian in the whole interest space. In the case of the filters with LMB birth distributions, this can produce at most one new track per time step. The single Gaussian distribution that covers the whole region of interest is given by $p_B^{(1)}(\mathbf{x}) = \mathcal{N}(\mathbf{x}; \mathbf{0}_{4\times 1}, \mathbf{\Sigma})$, where $\mathbf{\Sigma} = \text{diag}([707^2, 707^2, 10^2, 10^2])$. The reason for using this birth configuration is to show that using a Poisson distribution for the birth process enables the PMBM, PLMB and HPLMB filters to converge to the correct target state faster than the LMB and δ-GLMB filters when there are insufficient labeled Gaussian components comprising the LMB birth density.
2. An array of 5×5 Gaussian distributions in the interest space. This is equivalent to 25 labels in the case of LMB birth distributions (for the LMB and δ-GLMB filters), and a sum of Gaussians in the case of the Poisson birth distributions (for the PMBM, PLMB and HPLMB filters). The Gaussian distributions that cover the whole region of interest are given by $p_B^{(i)}(\mathbf{x}) = \mathcal{N}(\mathbf{x}; \mathbf{m}_i, \mathbf{\Sigma})$, where $\mathbf{\Sigma} = \text{diag}([235.5^2, 235.5^2, 10^2, 10^2])$ and $\{\mathbf{m}_1, ..., \mathbf{m}_{25}\} = g \times g$, where $g = [-666, -333, 0, 333, 666]^T$, all units being [m]. Under this birth configuration, a similar performance of all the tested filters is expected, since the Gaussian distributions cover the whole space, and the number of new targets frame by frame in the experiments never exceeds 25.
3. To provide a birth configuration that favors the use of an LMB birth model, 20 Gaussian distributions $p_B^{(i)}(\mathbf{x}) = \mathcal{N}(\mathbf{x}; \mathbf{m}_i, \mathbf{\Sigma}_i)$ are located at the positions where the ground truth targets initially appeared, i.e. the position components of $\mathbf{m}_i$ are located at the circles "$\circ$" in Fig. 1. The covariance matrix is diagonal with standard deviations of 10[m] for positions and 10[ms^{-1}] for the velocities. Therefore, $\mathbf{\Sigma}_i = \text{diag}([10^2, 10^2, 10^2, 10^2])\ \forall\ i \in \{1, ..., 20\}$. Under this artificial[4] configuration it is expected that the δ-GLMB and LMB filters should perform better than with birth configurations 1 and 2.

For all the three configurations, the Poisson birth intensity is given by $D_B(\mathbf{x}) = \lambda_B \sum_{i=1}^{N_B} \frac{1}{N_B} p_B^{(i)}(\mathbf{x})$, where the average target birth rate $\lambda_B = 0.15$ per scan, and N_B is the number of corresponding Gaussian distributions. The single target state of the LMB distribution is given by $p_B^{(i)}(\mathbf{x}, \ell) = p_B^{(i)}(\mathbf{x})\delta_{\ell_i}(\ell)$ with probability of existence $r_B = 0.15$ for all birth targets, where for label $\ell_i = (t, i)$, t is the time step and i is the index of the Gaussian distribution. Other parameters used in the filters are given in Table 2.

Although requiring a significant increase in computational time, a version of the δ-GLMB filter, referred to as δ-GLMB$_2$, is also tested with parameters: Number of iterations of the Gibbs sampler: $S = 10,000$; Limit on number of posterior components: $N^{\text{mb}} \leq 100,000$. This is to demonstrate that higher accuracy results are possible with the δ-GLMB filter, when the truncation of the posterior density is reduced, at the expense of greatly increased computational time. In the results, the processing time in this case is increased on average by a factor of 3 (see Fig. 5).

To account for the randomness of the system and measurement noises and the Gibbs sampling procedure, ten different measurement sets were randomly generated, and the filters where run ten times per measurement configuration. The results are the mean (and standard deviation) of these 100 tests.

As a proof of concept, Fig. 2a shows the resulting trajectories of one realization for the LMB filter (2a,c,e) and the HPLMB filter (2b,d,f), for birth configurations 1 to 3, respectively. In the Figure, different colors represent unique labels. In a qualitative sense, it can be seen that both the LMB and HPLMB filters show similar performances in terms of both label and trajectory estimation.

Comparing birth configuration 1 with 2 and 3, we observe that the LMB filter requires more time to estimate targets, particularly under birth configuration 1 (note the increased distances between the $\circ$ and the trajectory initializations). However this does not occur with the HPLMB filter, which is able to initiate target tracks very close to the beginning of their true trajectories under all three birth models. The performance of each filter under each birth scenario can also be quantified in terms of track deviation from ground truth. Therefore, Fig. 3 shows the OSPA and OSPA$^{(2)}$ metrics (cut-off $c = 100$[m], power $p = 2$ and for OSPA$^{(2)}$, the window $L = 10$[time steps]) and Fig. 4 shows the CLEAR MOT metrics for all birth configurations.

5.3. Filter Processing Times

Fig. 5 shows the average processing time of the filters for the three birth configurations. It is important to note that all filters were implemented in MATLAB, with the implementations of the LMB and δ-GLMB filters taken from [26]. The computational hardware characteristics are: Operating system Ubuntu 18.04; Processor Intel Core i7-4790; Memory 7.7 GB.

5.4. Analysis of the Results

It is important to note that, as expected, the LMB filter is faster than the δ-GLMB filter, and similarly the PLMB and HPLMB filters are faster than PMBM filter under all three birth scenarios. This is because the LMB, PLMB and HPLMB filters are single MB-component filters, while the δ-GLMB and PMBM filters are based on mixtures of MB components.

Birth Configuration 1: As expected, under birth configuration 1, the PLMB, HPLMB, LBP-PLMB and PMBM filters yield the best OSPA and OSPA$^{(2)}$ results. The Poisson birth based algorithms perform better than their LMB based counterparts because there is less delay in the number of time steps required to initialize new multiple tracks. In contrast, when the birth model is composed of a single Gaussian component, the LMB, LMBM and δ-GLMB filters can at most create one new target per time step. For example, at time step 20 when 9 new targets appear, the rate of reduction in the

[4] Since the ground truth initial location of the targets would not usually be known.

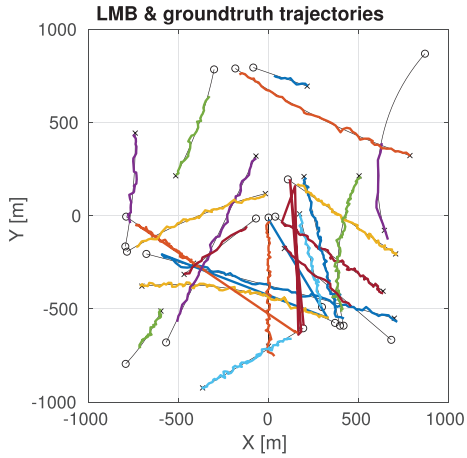

(a) Resulting trajectories using the LMB filter for birth model 1.

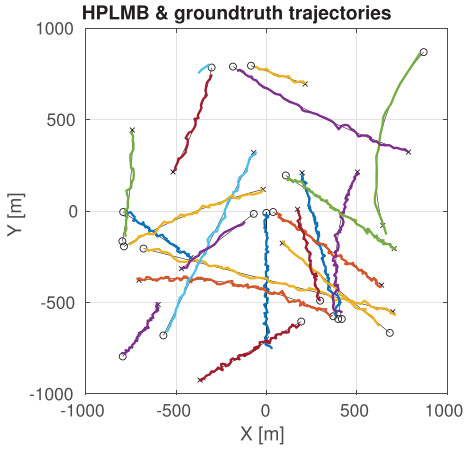

(b) Resulting trajectories using the HPLMB filter for birth model 1.

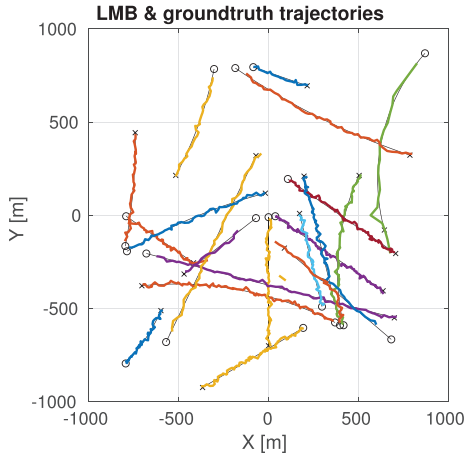

(c) Resulting trajectories using the LMB filter for birth model 2.

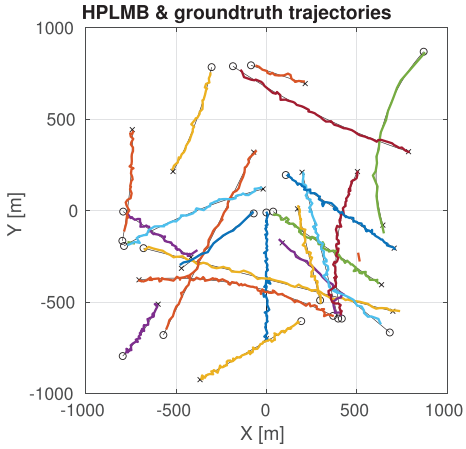

(d) Resulting trajectories using the HPLMB filter for birth model 2.

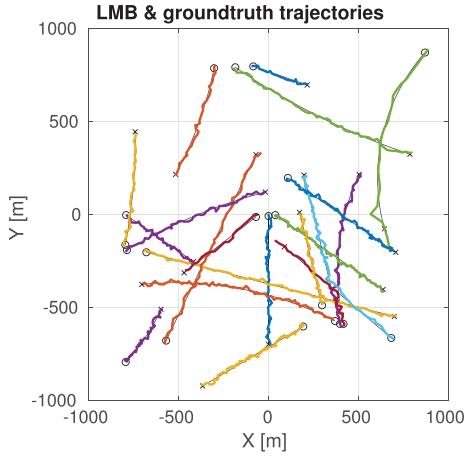

(e) Resulting trajectories using the LMB filter for birth model 3.

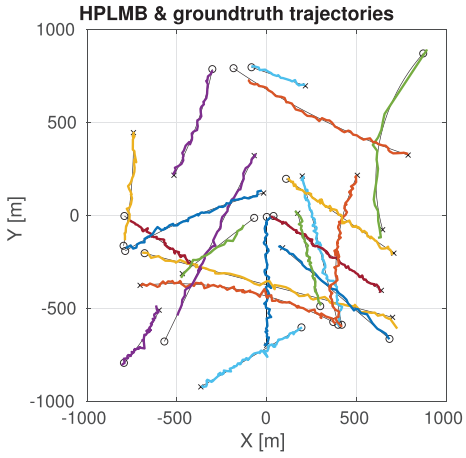

(f) Resulting trajectories using the HPLMB filter for birth model 3.

Fig. 2. Estimated trajectories for all the different tested birth models.

OSPA metric (Fig. 3) is significantly slower than that for the Poisson birth based filters. It should also be noted however that, for the LMB and δ-GLMB filters, since this birth configuration results in at most one new target per time step, they have lower computational times than the PLMB, HPLMB filters and PMBM filters, respectively. This is because the cost matrices, in the LMB and δ-GLMB filters, generate only one new hypothesis per time step. This is significantly less than the number generated in the PLMB, HPLMB and PMBM filters, in which one new hypothesis is created by each measurement per time step (i.e. more than 30 clutter

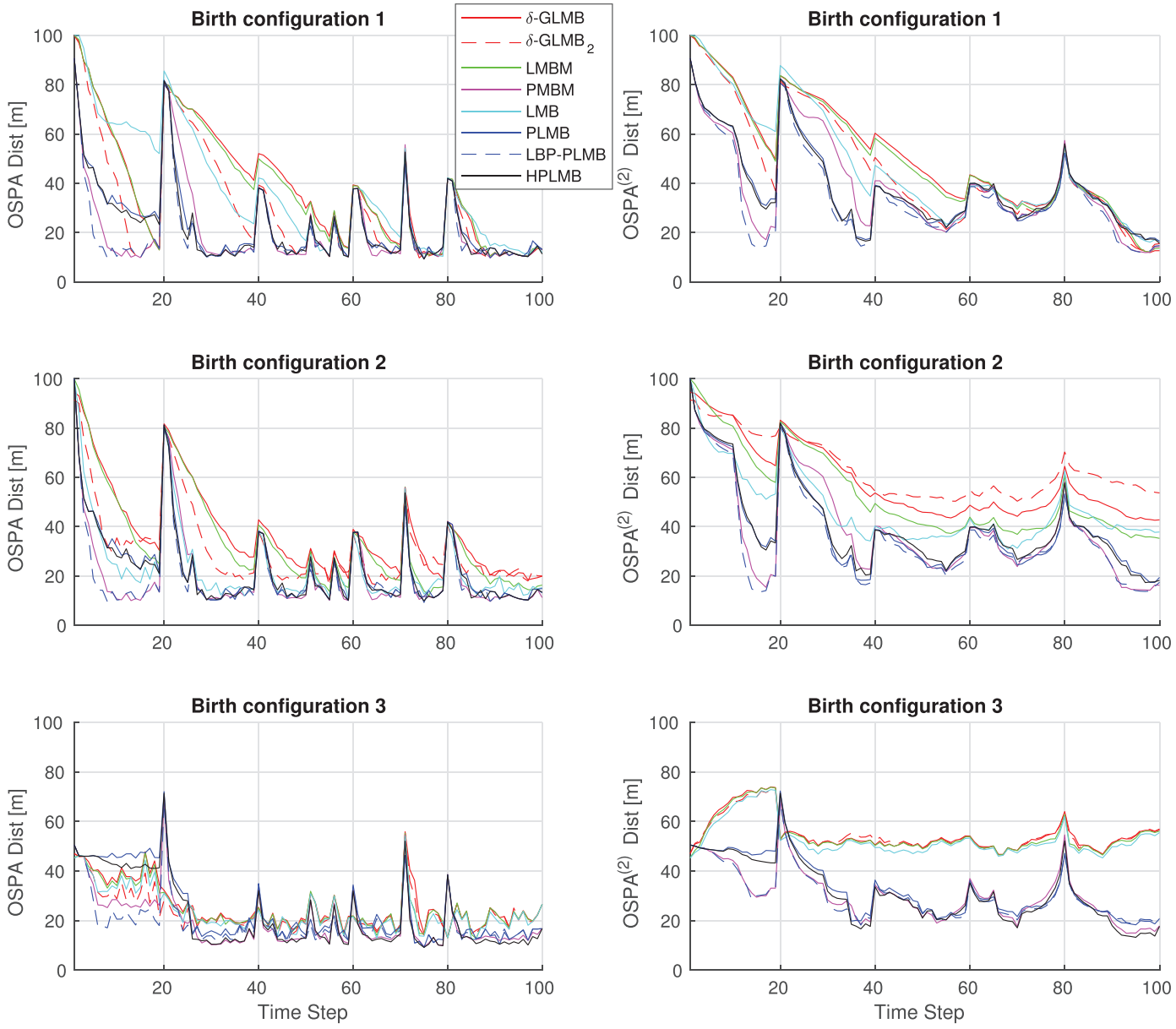

Fig. 3. OSPA (left) and OSPA$^{(2)}$ (right) metrics for all three birth configurations (1 to 3 from top to bottom respectively).

and true target based measurements per time step in this simulation). The new target hypotheses created as a result of clutter by the PLMB, HPLMB and PMBM filters will be updated but discarded rapidly because their probabilities of existence quickly reduce to a value lower than a threshold ("Threshold to prune tracks" in the list of parameters in Table 2).

Birth Configuration 2: In birth configuration 2, the LMB, LMBM and δ-GLMB filters improved with respect to configuration 1. The LMB filter achieved the same performance as the PMBM, PLMB, LBP-PLMB and HPLMB filters, and the MOTA metric value increased by 7% compared to configuration 1, which gives an indication of the fraction of total targets being tracked. This improvement is expected because the LMB filter uses 25 components for the birth process. This however makes the filter slower than under birth configuration 1. The PMBM, PLMB, LBP-PLMB and HPLMB filters performed similarly under a single Gaussian birth or with 25 Gaussian birth components covering the whole space.

The performance of the δ-GLMB filter under birth configuration 2 increased by 2% over that of birth configuration 1, with respect to the MOTA metric, however its performance is still below that of the other filters, by approximately 9%. A similar improvement is apparent in terms of the OSPA metric values. Comparing the performance of the δ-GLMB filter and δ-GLMB$_2$ filter (which uses more MB components), clear improvements in terms of the OSPA, MOTA and MOTP metrics are evident in Figs. 3 and 4. Note that to obtain comparable OSPA, OSPA$^{(2)}$, MOTA and MOTP performance values for the δ-GLMB filter and all the other tested filters, the higher number of MB components used in the δ-GLMB$_2$ filter were necessary. This comes at the expense of a significant increase in processing time, as shown in Fig. 5.

Birth Configuration 3: In birth configuration 3, where the birth Gaussians are artificially located in the positions at which the targets initially appear, all filters yield a more similar performance than under birth configurations 1 and 2 as expected. Surprisingly however, under this birth configuration, although the performance of each filter with respect to the OSPA metric appears similar, the

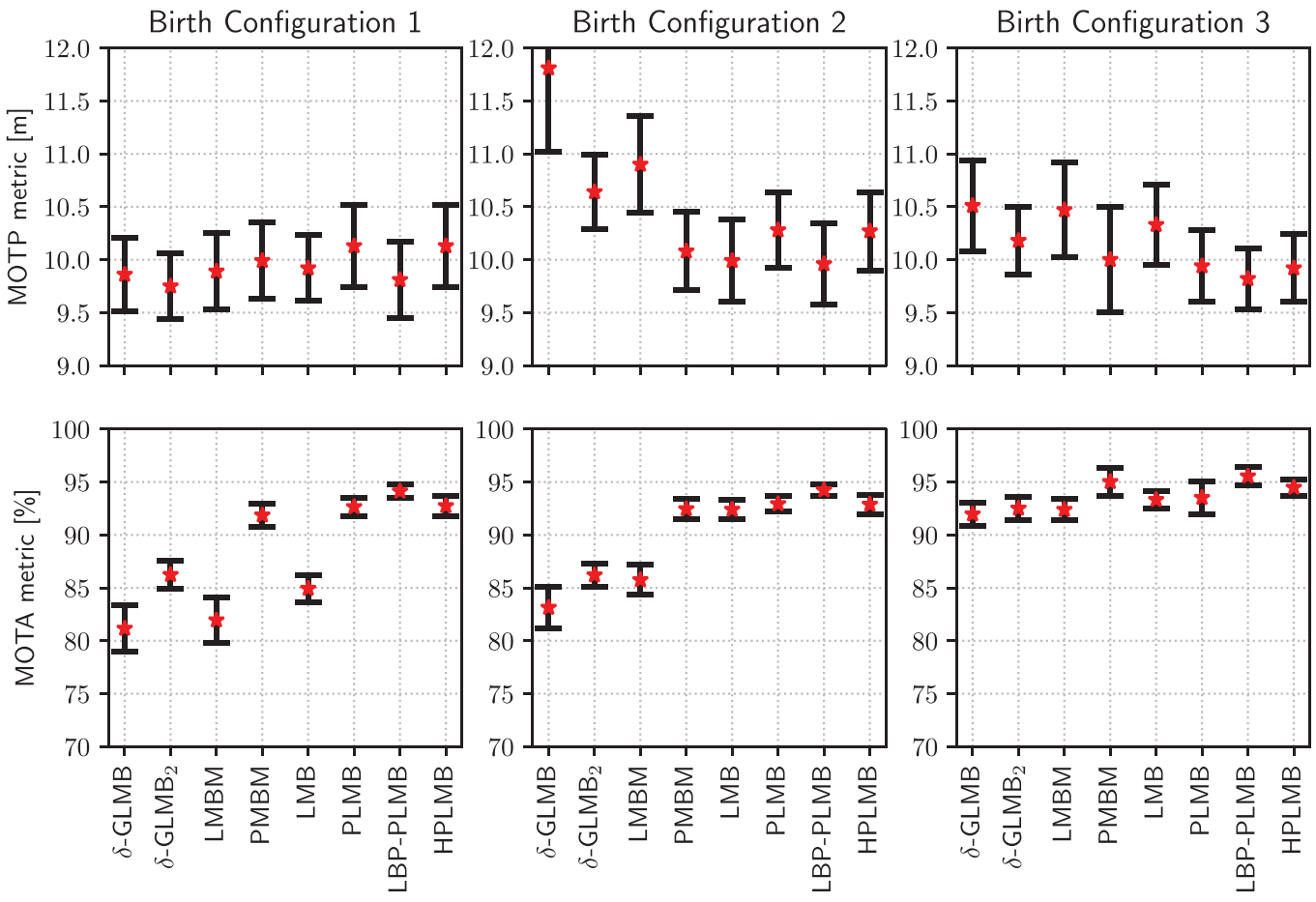

Fig. 4. CLEAR MOT metrics (MOTP and MOTA) for the three birth configurations. The graphs show the average (red stars) ± one standard deviation (black lines) of the 100 tests performed by each filter.

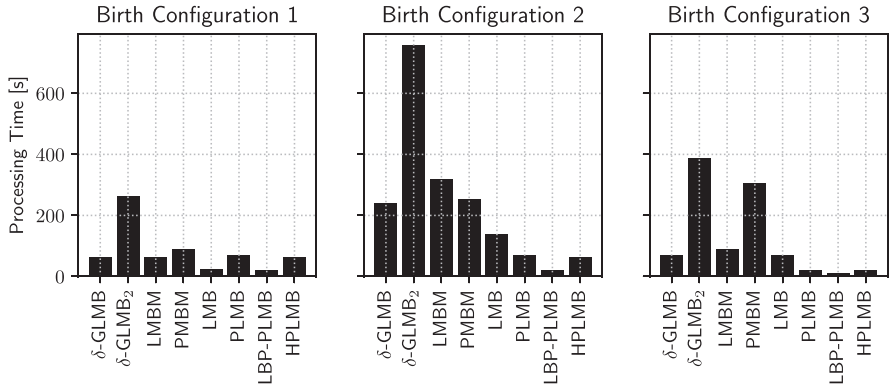

Fig. 5. Average processing time for the three birth configurations.

OSPA$^{(2)}$ and CLEAR MOTA metrics show higher performance of the Poisson birth model based filters.

5.4.1. Comparison of the different implementations of the PLMB Filter

The PLMB and HPLMB filters show very similar performances under all birth configurations. However, as shown in Fig. 5 the HPLMB filter is slightly faster than the PLMB filter due to the simpler implementation procedure of the HPLMB filter. This is because the HPLMB posterior is constructed directly from the histogram of Gibbs samples in Eqs. (43) to (45). However in the PLMB filter, the construction of the posterior requires each Gibbs sample to be stored, followed by the removal of repeated samples, before the resulting samples can be used to form the posterior given by Eqs. (42). This is at the expense of a very slight performance loss in terms of the MOTA metric.

Note that the LBP-PLMB filter is faster and more accurate than the Gibbs sampling based PLMB filter. It is faster because it has linear complexity in the number of measurements and targets, and needs fewer iterations to converge to the solution. It is more accurate because it is an optimization-based method that con-

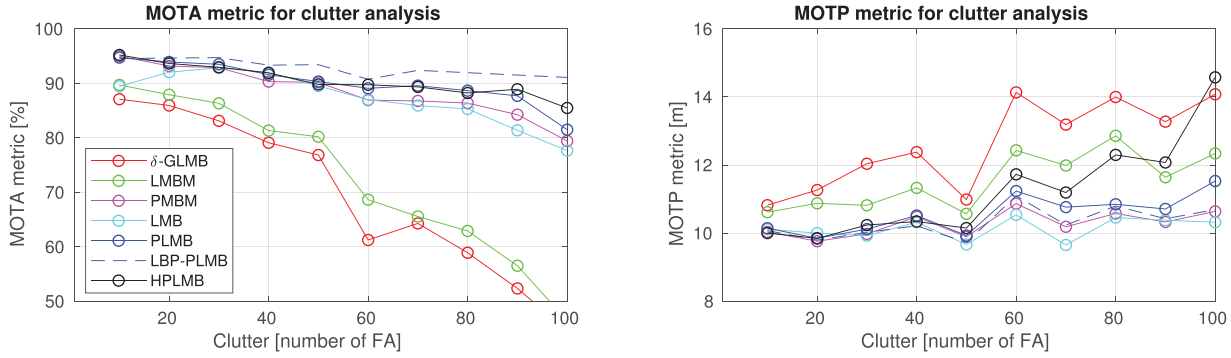

Fig. 6. CLEAR MOT metric values for all tested filters under birth configuration 2 (composed of an equally spaced Gaussian mixture), based on the following clutter rates: 10, 20, 30, 40, 50, 60, 70, 80, 90 and 100 false alarms per scan. The left figure shows the MOTA metric, and the right figure the MOTP metric.

verges to the importance value of the contribution of each prior-hypothesis and measurement association $h_{i,j}$. In contrast, Gibbs based sampling methods, truncate the posterior density. Gibbs sampling based target-measurement assignment methods however can be used in the PMBM, δ-GLMB, LMBM and other similar filters based on mixtures of MB densities.

5.4.2. Performance under different clutter rates

An experiment to measure the performance of the filters under different clutter rates is shown in Fig. 6, in terms of the CLEAR MOT metric. This is based on birth configuration 2, the configuration expected to result in the most equal performance of all filters.

As expected, all filters achieve a lower performance at higher clutter rates. In general, the δ-GLMB and LMBM filters perform worse than the other filters, all of which exhibit similar results. The proposed PLMB based filters (PLMB, LBP-PLMB and HPLMB filters) as well as the PMBM filter all create a new target hypotheses per measurement that could intuitively give rise to false track hypotheses. However if, over time, there are no new measurements to substantiate these hypotheses, they are discarded during the pruning process. Therefore, target hypotheses born from clutter measurements are rarely selected as target tracks by the state extraction method, which calculates the most likely cardinality N_{cd} of the posterior density and selects the N_{cd} target tracks with higher probabilities of existence.

6. Conclusions

This article introduced a sample based PLMB filter. The LMB density naturally results when applying Bayes theorem to a Poisson prior. The only assumption necessary when defining a Poisson prior is the expected number of targets in the region of interest. The PLMB filter is also intuitive since it models the existence probability of targets in a single MB density. It was also demonstrated that the PLMB filter approximates the PMBM filter in a manner analogous to the way the LMB filter approximates the δ-GLMB filter maintaining the same advantages and disadvantages. It was also shown that the PLMB filter is capable of tracking targets as accurately as the LMB filter, with comparable computational complexity, when the PHD of the LMB birth model is equal to that of the Poisson birth model. The PLMB filter demonstrates a superior performance over its LMB filter counterpart, when the birth model cardinality hypothesis is less than the number of measurements. The PLMB filter has a more consistent performance under different birth distribution configurations compared to the LMB filter. A histogram based Gibbs sampling method was also proposed, that directly calculates the posterior PLMB distribution. Using the Gibbs sampling approach, the weight based PLMB filter requires the removal of repeated sampled MB components, whereas the HPLMB filter does not.

Results show that the LBP method performs faster and with higher accuracy than the Gibbs-based implementation of the proposed PLMB filter since the Gibbs-based target-measurement assignment truncates the posterior density whereas the LBP algorithm iterates until to an acceptable error is reached. In contrast to the LBP approach, the histogram-Gibbs sampling approach demonstrated in the HPLMB filter, can also be implemented in other MB-based filters and it is of interest to apply it in the δ-GLMB, LMBM, PMBM and LMB filters.

Declaration of Competing Interest

The authors declare that they have no known competing financial interests or personal relationships that could have appeared to influence the work reported in this paper.

Acknowledgement

This research was partially funded by the US Air Force Office of Scientific Research, under award number FA9550-17-1-0386. The work was also partially funded by CONICYT/PIA Project AFB180004 and Conicyt, Fondecyt Projects 1190979 and 3180319.

Appendix A

Derivation of Equation (18). The PGFl of the prior distribution (after prediction), is of the form:

$$G^{+}_{\mathcal{X}|\mathcal{Z}}[h] = \underbrace{e^{\langle D_{\mathcal{B}}(\mathbf{x}),h(\mathbf{x})-1\rangle}}_{G_{\mathcal{B}|\mathcal{Z}}[h]} \times \underbrace{\prod_{\ell\in L} 1-r'_{\ell}+r'_{\ell}\langle f'_{\ell}(\mathbf{x}),h(\mathbf{x})\rangle}_{G'_{\mathcal{Y}|\mathcal{Z}}[h]}, \tag{48}$$

where Y is the set of existing targets, B the set of new targets, and $G_{\mathcal{B}|\mathcal{Z}}[h]$ and $G'_{\mathcal{Y}|\mathcal{Z}}[h]$ their respective PGFl.

The Poisson distribution models new targets such that no detection probability, P_D, is needed (equivalent to setting $P_D = 1$). By using the standard observation model, the joint PGFl is defined as follows:

$$\begin{aligned} F[g,h] &= G_{\Phi}[g]G_{\mathcal{B}|\mathcal{Z}}[h\langle l_z(\cdot|\cdot),g\rangle]G'_{\mathcal{Y}|\mathcal{Z}}[h(1-P_D+P_D\langle l_z(\cdot|\cdot),g\rangle)] \\ &= e^{\langle D_{\Phi},g-1\rangle}e^{\langle D_{\mathcal{B}},h\langle l_z(\cdot|\cdot),g\rangle-1\rangle} \\ &\quad\times\prod_{\ell\in L} 1-r'_{\ell}+r'_{\ell}\langle(1-P_D+P_D\langle l_z(\cdot|\cdot),g\rangle)f_{\ell}',h\rangle. \end{aligned} \tag{49}$$

Differentiating with respect to Z gives:

$$\frac{\delta}{\delta Z}F[g,h] = \frac{\delta}{\delta Z}\Bigg\{ e^{\langle D_{\Phi},g-1\rangle+\langle D_{\mathcal{B}},h\langle l_z(\cdot|\cdot),g\rangle-1\rangle}$$

$$\times \prod_{\ell\in L} 1 - r'_\ell + r'_\ell \langle (1 - P_D + P_D \langle l_z(\cdot|\cdot), g\rangle) f'_\ell, h\rangle \Big\}. \quad (50)$$

This can be evaluated using the product rule for set derivatives [8, p.395]:

$$\frac{\delta}{\delta X} \prod_i^n F_i = \sum_{X_1 \uplus \cdots \uplus X_n = X} \prod_i^n \frac{\delta}{\delta X_i} F_i, \quad (51)$$

resulting in:

$$\frac{\delta}{\delta Z} F[g,h] = \sum_{Z_0 \uplus \cdots \uplus Z_n = Z} \frac{\delta}{\delta Z_0} \left\{ e^{\langle D_\Phi, g-1\rangle + \langle D_\mathcal{B}, h\langle l_z(\cdot|\cdot), g\rangle - 1\rangle} \right\} \times \prod_{\ell\in L} \frac{\delta}{\delta Z_{j_\ell}} \left\{ 1 - r'_\ell + r'_\ell \langle (1 - P_D + P_D \langle l_z(\cdot|\cdot), g\rangle) f'_\ell, h\rangle \right\}, \quad (52)$$

with $Z_0 \uplus Z_1 \uplus \cdots \uplus Z_n$ being a partition of the observation set Z.

The derivative of the exponential term can be calculated as follows:

$$\begin{aligned} \frac{\delta}{\delta\{\mathbf{z}_1, \ldots, \mathbf{z}_{m^0}\}} \{\ldots\} &= D_\Phi(\mathbf{z}_1) + \langle D_\mathcal{B}, h l_z(\mathbf{z}_1|\cdot) - 1\rangle \times \frac{\delta}{\delta\{\mathbf{z}_2, \ldots, \mathbf{z}_{m^0}\}} \{\ldots\} \\ &\vdots \\ &= e^{\langle D_\Phi, g-1\rangle + \langle D_\mathcal{B}, h\langle l_z(\cdot|\cdot), g\rangle - 1\rangle} \\ &\quad \times \prod_{\mathbf{z}\in Z_0} D_\Phi(\mathbf{z}) + \langle D_\mathcal{B}, h l_z(\mathbf{z}|\cdot) - 1\rangle. \end{aligned} \quad (53)$$

Using the fact that the derivative of a linear operator has non-zero values only for the empty set and a singleton (see [8, p.395]), sets Z_1 to Z_n can have zero or one element only. Thus, it is possible to identify the derivatives with respect to singletons and with respect to the empty set:

$$\begin{aligned} &\prod_{\ell\in L} \frac{\delta}{\delta Z_j} \{\ldots\} = \prod_{\ell^D} \frac{\delta}{\delta\{\mathbf{z}_j\}} \left\{ 1 - r'_{\ell^D} + r'_{\ell^D} \langle (1 - P_D + P_D \langle l_z(\cdot|\cdot), g\rangle) f'_{\ell^D}, h\rangle \right\} \\ &\quad \times \prod_{\ell^M} \frac{\delta}{\delta\emptyset} \left\{ 1 - r'_{\ell^M} + r'_{\ell^M} \langle (1 - P_D + P_D \langle l_z(\cdot|\cdot), g\rangle) f'_{\ell^M}, h\rangle \right\} \\ &= \prod_{\ell^D} r'_{\ell^D} \langle P_D l_z(\mathbf{z}_j|\cdot) f'_{\ell^D}, h\rangle \times \prod_{\ell^M} 1 - r'_{\ell^M} \\ &\quad + r'_{\ell^M} \langle (1 - P_D + P_D \langle l_z(\cdot|\cdot), g\rangle) f'_{\ell^M}, h\rangle, \end{aligned} \quad (54)$$

where $\ell^D \in L^D$ are subsets of the label set L that are paired with measurements, whereas $\ell^M \in L^M$ are subsets of L that are not assigned any measurement (misdetected). This yields $F[g, h]$ as follows:

$$\begin{aligned} \frac{\delta}{\delta Z} F[g,h] &= e^{\langle D_\Phi, g-1\rangle + \langle D_\mathcal{B}, h\langle l_z(\cdot|\cdot), g\rangle - 1\rangle} \\ &\quad \times \sum_\sigma \left(\prod_{\mathbf{z}\in Z_0} D_\Phi(\mathbf{z}) + \langle D_\mathcal{B} l_z(\mathbf{z}|\cdot), h\rangle \right) \\ &\quad \times \left(\prod_{\ell^D\in L^D} r'_{\ell^D} \langle P_D l_z(\mathbf{z}_j|\cdot) f'_{\ell^D}, h\rangle \right) \\ &\quad \times \left(\prod_{\ell^M\in L^M} 1 - r'_{\ell^M} + r'_{\ell^M} \langle (1 - P_D + P_D \langle l_z(\cdot|\cdot), g\rangle) f'_{\ell^M}, h\rangle \right). \end{aligned} \quad (55)$$

Evaluating at $g = 0$ results in:

$$\begin{aligned} \frac{\delta}{\delta Z} F[g,h]\Big|_{g=0} &= e^{\langle D_\Phi, -1\rangle + \langle D_\mathcal{B}, -1\rangle} \times \sum_\sigma \underbrace{\prod_{\mathbf{z}\in Z_0} D_\Phi(\mathbf{z}) + \langle D_\mathcal{B} l_z(\mathbf{z}|\cdot), h\rangle}_{f_N^u[h]} \\ &\quad \times \underbrace{\prod_{\ell^D\in L^D} r'_{\ell^D} \langle P_D l_z(\mathbf{z}_j|\cdot) f'_{\ell^D}, h\rangle}_{f_D^u[h]} \times \underbrace{\prod_{\ell^M\in L^M} 1 - r'_{\ell^M} + r'_{\ell^M} \langle (1 - P_D) f'_{\ell^M}, h\rangle}_{f_M^u[h]}, \end{aligned} \quad (56)$$

where the terms $f^u[h]$ are unnormalized MB components. The unnormalized MB components can be rewritten as MB distributions multiplied by a weighting factor as follows:

$$\begin{aligned} a + b < g, h > &= w(1 - r + r < f, h >), \quad \text{with } f = \frac{g}{\langle g, 1\rangle}, \\ r = \frac{\langle g, 1\rangle b}{a + \langle g, 1\rangle b}, &\quad w = a + \langle g, 1\rangle b, \end{aligned} \quad (57)$$

where a and b are the parameters of the unnormalized MB component, and ω and r are the parameters of the equivalent MB distribution.

Distinct labels $\ell^N \in L^N$ are added to hypotheses arising from each measurement $\mathbf{z} \in Z_0$ by using a likelihood function $l_z(\mathbf{z}|\mathbf{x}, \ell) = l_z(\mathbf{z}|\mathbf{x})\delta_{\ell'}(\ell)$, corresponding to measurement $\mathbf{z}_j$ producing new target label $\ell^N = (t, j)$.

Using Eq. (58), $f_N^u[h]$ can be expressed in terms of the parameters of the posterior density $f^+_{\ell^N,N}$ and $r^+_{\ell^N,N}$, as follows:

$$f_N^u[h] = \underbrace{\prod_{\ell^N\in L^N} D_\Phi(\mathbf{z}_j) + \langle D_\mathcal{B} l_z(\mathbf{z}_j|\cdot), 1\rangle}_{\omega_N} \underbrace{\prod_{\ell^N\in L^N} 1 - r^+_{\ell^N,N} + r^+_{\ell^N,N} \langle f^+_{\ell^N,N}, h\rangle}_{f_N^{\text{lmb}}[h]}, \quad (58)$$

$$f^+_{\ell^N,N}(\mathbf{x}, \ell) = \frac{D(\mathbf{x}) l_z(\mathbf{z}_j|\mathbf{x}) \delta_{\ell^N}(\ell)}{\langle D_\mathcal{B} l_z(\mathbf{z}_j|\cdot), 1\rangle}, \quad r^+_{\ell^N,N} = \frac{\langle D_\mathcal{B} l_z(\mathbf{z}_j|\cdot), 1\rangle}{D_\Phi(\mathbf{z}_j) + \langle D_\mathcal{B} l_z(\mathbf{z}_j|\cdot), 1\rangle} \quad (59)$$

Similarly, $f_D^u[h]$ can be expressed in terms of $f^+_{\ell^D,j}$ and $r^+_{\ell^D,j}$, for a label ℓ^D detected by the measurement j:

$$f_D^u[h] = \underbrace{\prod_{\ell^D\in L^D} r'_{\ell^D} \langle P_D l_z(\mathbf{z}_j|\cdot) f'_{\ell^D}, 1\rangle}_{\omega_D} \underbrace{\prod_{\ell^D\in L^D} 1 - r^+_{\ell^D,j} + r^+_{\ell^D,j} \langle f^+_{\ell^D,j}, h\rangle}_{f_D^{\text{lmb}}[h]}, \quad (60)$$

$$f^+_{\ell^D,j}(\mathbf{x}, \ell) = \frac{P_D(\mathbf{x}, \ell) l_z(\mathbf{z}_j|\mathbf{x}, \ell) f'_{\ell^D}(\mathbf{x}, \ell)}{\langle P_D l_z(\mathbf{z}_j|\cdot) f'_{\ell^D}, 1\rangle}, \quad r^+_{\ell^D,j} = 1 \quad (61)$$

Finally, $f_M^u[h]$ can be expressed in terms of the posterior MB density parameters $f^+_{\ell^M,0}$ and $r^+_{\ell^M,0}$ as:

$$f_M^u[h] = \underbrace{\prod_{\ell^M\in L^M} 1 - r'_{\ell^M} + r'_{\ell^M} \langle (1 - P_D) f'_{\ell^M}, 1\rangle}_{\omega_M} \underbrace{\prod_{\ell^M\in L^M} 1 - r^+_{\ell^M,0} + r^+_{\ell^M,0} \langle f^+_{\ell^M,0}, h\rangle}_{f_M^{\text{lmb}}[h]}, \quad (62)$$

$$f^+_{\ell^M,0}(\mathbf{x}, \ell) = \frac{(1 - P_D(\mathbf{x}, \ell)) f'_{\ell^M}(\mathbf{x}, \ell)}{\langle (1 - P_D) f'_{\ell^M}, 1\rangle}, \quad r^+_{\ell^M,0} = \frac{\langle (1 - P_D) f'_{\ell^M}, 1\rangle r'_{\ell^M}}{1 - r'_{\ell^M} + \langle (1 - P_D) f'_{\ell^M}, 1\rangle r'_{\ell^M}}. \quad (63)$$

Thus, Eq. (56) can be rewritten as:

$$\frac{\delta}{\delta Z} F[g,h]\Big|_{g=0} = e^{\langle D_\Phi, -1\rangle + \langle D_\mathcal{B}, -1\rangle} \times \sum_\sigma \omega_N \omega_D \omega_M f_N^{\text{lmb}}[h] f_D^{\text{lmb}}[h] f_M^{\text{lmb}}[h]. \quad (64)$$

Remembering that:

$$G^{+}_{\mathcal{X}|\mathcal{Z}}[h] = \frac{\frac{\delta}{\delta Z}F[g,h]\big|_{g=0}}{\frac{\delta}{\delta Z}F[g,h]\big|_{g=0,h=1}},$$

which acts as a normalization constant, the final form of the PGFl for the corrected labeled multi-Bernoulli mixture posterior is:

$$G^{+}_{\mathcal{X}|\mathcal{Z}}[h] = \frac{1}{C}\sum_{\sigma}\omega_N\omega_D\omega_M f_N^{\text{lmb}}[h]f_D^{\text{lmb}}[h]f_M^{\text{lmb}}[h], \tag{65}$$

with C being a normalization constant such that all weights sum to unity. □

References

[1] C.S. Lee, D.E. Clark, J. Salvi, Slam with dynamic targets via single-cluster phd filtering, IEEE Journal of Selected Topics in Signal Processing 7 (3) (2013) 543–552.

[2] J. Mullane, B.-N. Vo, M.D. Adams, B.-T. Vo, A random-finite-set approach to bayesian slam, IEEE Transactions on Robotics 27 (2) (2011) 268–282.

[3] K.Y. Leung, F. Inostroza, M. Adams, Generalizing random-vector slam with random finite sets, in: Robotics and Automation (ICRA), 2015 IEEE International Conference on, IEEE, 2015, pp. 4583–4588.

[4] F. Zhang, H. Stähle, A. Gaschler, C. Buckl, A. Knoll, Single camera visual odometry based on random finite set statistics, in: Intelligent Robots and Systems (IROS), 2012 IEEE/RSJ International Conference on, IEEE, 2012, pp. 559–566.

[5] B.-N. Vo, M. Mallick, Y. Bar-shalom, S. Coraluppi, R. Osborne III, R. Mahler, B.-t. Vo, Multitarget tracking, Wiley Encyclopedia of Electrical and Electronics Engineering (1999) 1–15.

[6] R. Danchick, G.E. Newnam, A fast method for finding the exact n-best hypotheses for multitarget tracking, IEEE Transactions on Aerospace and Electronic Systems 29 (2) (1993) 555–560.

[7] I.J. Cox, S.L. Hingorani, An efficient implementation of reid's multiple hypothesis tracking algorithm and its evaluation for the purpose of visual tracking, IEEE Transactions on pattern analysis and machine intelligence 18 (2) (1996) 138–150.

[8] R. Mahler, Statistical Multisource-Multitarget Information Fusion, Artech House, Norwood, MA, USA, 2007.

[9] R. Mahler, Advances in Statistical Multisource-Multitarget Information Fusion, Artech House, Norwood, MA, USA, 2014.

[10] B.-T. Vo, B.-N. Vo, Labeled Random Finite Sets and Multi-Object Conjugate Priors, IEEE Transactions on Signal Processing 61 (13) (2013) 3460–3475.

[11] B.-N. Vo, B.-T. Vo, D. Phung, Labeled random finite sets and the bayes multi-target tracking filter, IEEE Transactions on Signal Processing 62 (24) (2014) 6554–6567, doi:10.1109/TSP.2014.2364014.

[12] K.G. Murty, An Algorithm for Ranking all the Assignments in Order of Increasing Cost, Operations Research 16 (3) (1968) 682–687, doi:10.1287/opre.16.3.682.

[13] B.-N. Vo, B.-T. Vo, H.G. Hoang, An efficient implementation of the generalized labeled multi-bernoulli filter, IEEE Transactions on Signal Processing 65 (8) (2017) 1975–1987.

[14] S. Reuter, B.-T. Vo, B.-N. Vo, K. Dietmayer, The Labeled Multi-Bernoulli Filter, IEEE Transactions on Signal Processing 62 (12) (2014) 3246–3260.

[15] S. Reuter, A. Danzer, M. Stübler, A. Scheel, K. Granström, A fast implementation of the labeled multi-Bernoulli filter using Gibbs sampling, in: Intelligent Vehicles Symposium (IV), 2017 IEEE, IEEE, 2017, pp. 765–772.

[16] T. Kropfreiter, F. Meyer, F. Hlawatsch, A fast labeled multi-Bernoulli filter using belief propagation, IEEE Transactions on Aerospace and Electronic Systems (2019), doi:10.1109/TAES.2019.2941104.

[17] J.L. Williams, An efficient, variational approximation of the best fitting multi--Bernoulli filter, IEEE Transactions on Signal Processing 63 (1) (2014) 258–273.

[18] J.L. Williams, Marginal multi-Bernoulli filters: RFS derivation of MHT, JIPDA, and association-based MeMBer, IEEE Transactions on Aerospace and Electronic Systems 51 (3) (2015) 1664–1687.

[19] J. Correa, M. Adams, C. Perez, A dirac delta mixture-based random finite set filter, in: International Conference on Control, Automation and Information Sciences (ICCAIS), 2015, pp. 231–238.

[20] Á.F. García-Fernández, J.L. Williams, K. Granstrom, L. Svensson, Poisson multi--Bernoulli mixture filter: direct derivation and implementation, IEEE Transactions on Aerospace and Electronic Systems 54 (4) (2018) 1883–1901.

[21] R. Mahler, Exact closed-form multi target bayes filters, Sensors 19 (12) (2019) 2818.

[22] S. Lin, B.T. Vo, S.E. Nordholm, Measurement driven birth model for the generalized labeled multi-Bernoulli filter, in: 2016 International Conference on Control, Automation and Information Sciences (ICCAIS), IEEE, 2016, pp. 94–99.

[23] L. Cament, M. Adams, J. Correa, A multi-sensor, Gibbs sampled, implementation of the multi-Bernoulli poisson filter, in: 2018 21st International Conference on Information Fusion (FUSION), IEEE, 2018, pp. 2580–2587.

[24] R. Mahler, On CPHD filters with track labeling, in: Signal Processing, Sensor/Information Fusion, and Target Recognition XXVI, 10200, International Society for Optics and Photonics, 2017, p. 102000E.

[25] H.W. Kuhn, The hungarian method for the assignment problem, Naval research logistics quarterly 2 (1-2) (1955) 83–97.

[26] Matlab RFS based multi-target filters, 2019, (http://ba-tuong.vo-au.com/codes.html) Accessed: 2019-12-02.

[27] Y. Xia, K. Granstrcom, L. Svensson, .F. García-Fernández, Performance evaluation of multi-bernoulli conjugate priors for multi-target filtering, in: 2017 20th International Conference on Information Fusion (Fusion), IEEE, 2017, pp. 1–8.

[28] D. Schuhmacher, B.-T. Vo, B.-N. Vo, A Consistent Metric for Performance Evaluation of Multi-Object Filters, IEEE Transactions on Signal Processing 56 (8) (2008) 3447–3457, doi:10.1109/TSP.2008.920469.

[29] M. Beard, B.T. Vo, B.-N. Vo, OSPA (2): Using the OSPA metric to evaluate multi-target tracking performance, in: 2017 International Conference on Control, Automation and Information Sciences (ICCAIS), IEEE, 2017, pp. 86–91.

[30] K. Bernardin, R. Stiefelhagen, Evaluating multiple object tracking performance: the CLEAR MOT metrics, Journal on Image and Video Processing 2008 (2008).